

Computation Reduction for Angle of Arrival Estimation Based on Interferometer Principle

by

Mukul Chandail

A thesis
presented to the University of Waterloo
in fulfillment of the
thesis requirement for the degree of
Master of Applied Science
in
Electrical and Computer Engineering

Waterloo, Ontario, Canada, 2017

© Mukul Chandail 2017

Author's Declaration

I hereby declare that I am the sole author of this thesis. This is a true copy of the thesis, including any required final revisions, as accepted by my examiners.

I understand that my thesis may be made electronically available to the public.

Abstract

Advancement in wireless technology and the oncoming of the Internet of Things (IoT) marked an incredible growth in the wireless connectivity, ultimately concluding in a major expansion in the mobile electronics industry. Today, around 3.1 billion users are reported being connected to the internet, along with 16.3 billion mobile electronic devices. The increasing connectivity has led to an increase in demand for mobile services, consequently, increasing demand for location services and mobility analytics. The most common location tracking or direction finding devices are found in the form of Global Positioning System (GPS) which provides location data for a client device using satellite-based lateration techniques. However, the use of the GPS is fairly limited to large distances and often tends to fail when smaller distances are concerned. This thesis aims to dive into the study of different direction finding algorithms based on angle of arrival estimation specifically pertaining to the indoor location tracking and navigation, also known as hyperlocation. The thesis will go over the main elements used in direction finding systems while looking at some of the present research done in this respective field of interest. Afterwards, the thesis will focus on a specific angle of arrival estimation algorithm which is widely being used for hyperlocation solutions and propose an alteration in the algorithm in order to achieve a faster runtime performance on weaker processors. A comparison between the accuracies will be made between the original algorithm and the suggested solution, followed by a runtime comparison on different processing units.

Acknowledgements

I would like to thank Cisco Systems for sponsoring my research and providing me the opportunity of working with them as a summer intern, thereby introducing me to the world of direction finding and hyperlocation.

I would also like to thank my manager and supervisor Paul Stager for his indispensable guidance and mentorship throughout my internship. Without Pauls direction, none of this would have been possible. Finally, I would like to thank my supervisors Dr. Gordon Agnew and Dr. Wojciech Golab for all their support and help throughout my course of study at the University of Waterloo.

Dedication

This thesis is dedicated to those aiming at reducing complexity in this overly complex world.

Table of Contents

List of Tables	ix
List of Figures	x
1 Introduction	1
1.1 Motivation	2
1.2 Purpose	3
1.2.1 Cell of Origin	3
1.2.2 Distance Based (Lateration) Techniques	3
1.2.3 Angle-Based (Angulation) or Angle of Arrival (AoA) Techniques	4
1.3 Problem Statement	4
1.4 Thesis Organization	5
2 Background	6
2.1 Direction Finding	6
2.1.1 Overview	6
2.1.2 Applications of direction finding	8
2.1.3 Passive direction finding	8
2.2 Bearings	9
2.2.1 Overview	9
2.2.2 Angle of Arrival	10

2.3	Time Difference of Arrival (TDoA)	13
2.4	Received Signal Strength Indicator (RSSI)	15
2.5	Amplitude Comparison	16
3	Literature Review	18
3.1	Triangulation Method - Rotating Beacons	18
3.2	Cooperative AoA Localization Scheme (CALs)	21
3.3	Digital Beamforming Approach	21
3.3.1	Bartlett	23
3.3.2	Capon	23
3.3.3	MUSIC	24
3.4	Performance Evaluation	24
4	Digital Beamforming and Direction Finding	26
4.1	Antenna Radiation Patterns	26
4.2	Directional Antenna Array	27
4.2.1	Directional Antennas	27
4.2.2	Array Antennas	29
4.2.3	Linear Array	30
4.2.4	Circular Array	33
4.3	Digital Beamforming	35
4.4	Correlative Interferometry	36
4.5	Direction finding Algorithm using Planar sweep	38
4.5.1	Obtaining the measured phase vector	39
4.5.2	Calculating ideal phase vector	40
4.5.3	Calculating the Correlation Matrix	42
4.6	Direction finding Algorithm Using Spherical Sweep	42
4.7	Refining Results	43
4.7.1	Coarse Search and Fine Search	43
4.7.2	Interpolation approach	45

5	Evaluation	47
5.1	Antenna Array Geometry	47
5.1.1	Circular Array - 8 Elements	48
5.1.2	Circular Ring Antenna Array - 16 Elements	49
5.1.3	Circular Antenna Array - 32 Elements	50
5.1.4	Square Antenna Array - 16 Elements	51
5.1.5	Halo Antenna Array 32 Elements	52
5.2	Performance Analysis	53
5.3	Runtime Comparison	57
6	Conclusion	59
6.1	Future Work	60
	References	61

List of Tables

5.1	Comparison between azimuth angle values computed using interpolation method for different antenna arrays.	54
5.2	Comparison between elevation angle values computed using interpolation method for different antenna arrays.	55
5.3	Comparison of both azimuth and elevation angle generated by planar sweep using resolution 200x200 and 50x50.	56
5.4	Runtime comparison between planar sweep and interpolation algorithm on different processing units.	58

List of Figures

2.1	Triangulation scheme.	7
2.2	Flow of information in direction finding system.	8
2.3	Bearings depicted by lines AB and BA in the south-west and north-east direction.	10
2.4	Azimuth and Elevation angles.	12
2.5	CISCO's HALO Antenna[22].	13
2.6	Two-antenna system.	14
2.7	Two antenna with boresights offset by 90 degrees.	17
3.1	System Model.	19
3.2	Triangulation and Trilateration	20
3.3	General scheme of AoA system	22
4.1	Antenna radiation pattern in Polar and Cartesian coordinates[16]	27
4.2	Radiation pattern of a Directional Antenna	29
4.3	Uniformly Spaced Linear Array	31
4.4	Eight element linear array pattern	33
4.5	Circular Antenna Array	34
4.6	Circular array pattern[11].	35
4.7	Correlation matrix and correlation function.	38
4.8	Azimuth sweep.	40

4.9	Azimuth and Elevation Sweep	42
4.10	Hemi-spherical sweep.	43
4.11	Correlation plot for coarse search.	44
4.12	Correlation plot for fine search.	45
4.13	Inverted parabola.	46
5.1	Circular Antenna Array - Circular8	48
5.2	Circular Ring	49
5.3	Circular antenna Array (Circular32)	50
5.4	Square Antenna Array	51
5.5	Halo Antenna Array	52

Chapter 1

Introduction

After the scientific revolution brought in by the World War II to the communication sector, the use of radar became more widespread among both the civilian and military services. Initially, the radar systems were designed to gather information about distant objects, such as vehicles, aircraft, submarines, etc. These systems used to emit electromagnetic waves; and based on the returning reflections of those waves, the location and velocity of the distant objects were determined. With passing time, improvements in the radar systems, introduction of directional antennas, and wireless technology gave birth to Radio Direction Finding (RDF). Radio direction finders work by capturing two or more measurements of the same signal, and then locate the signals source using the marginal differences between those points. Almost every direction finding system uses the time of the incoming signal arrival (ToA), the angle of the incoming signal arrival (AoA), or the received power of the incoming signal, i.e. Received Signal Strength Indicator (RSSI) as the indicators for localization. Today, direction finding techniques have found applications in air traffic surveillance, navigation of ships and aircraft, locating hidden transmitters, etc. Despite the brief evolution, the rapid growth in the area of the Wi-Fi technology and wireless networks is opening a new dimension in the research and development for the direction finding systems by laying focus on indoor navigation. This avenue is marked under the term of Hyperlocation, promising an inevitable growth in the methodologies for direction finding.

1.1 Motivation

With the unprecedented growth of Wi-Fi technology and the demand for wireless connectivity, portable electronic devices like smart phones and tablets have become a common place thing. More and more individuals now have access to these portable devices, increasing the numbers of individuals connected to the internet. Based on Cisco's Visual Networking Index (VNI), total internet traffic has experienced dramatic growth in the past two decades. By the end of the year 2016, 3.1 billion users were reported being connected to the internet, with 16.3 billion connected electronic devices. Cisco predicts these numbers to grow further by the year 2020 with over 1.1 billion new internet users, and 10 billion new connected devices. The growth of smartphones as the communications hub for social media, video consumption, tracking Internet of Everything (IoE) applications demonstrates the effect that smartphones have on consumers and businesses users access across the internet and IP networks [17].

The increasing user connectivity to the Internet of Things (IoT) has led to an increasing demand in the user mobility analytics and location tracking. This is evident from the rise of the Global Position System (GPS) devices, and location tracking services like Google Maps, Apple Maps, etc. However, these location technologies use the satellite services for location tracking on a large area. As a result, they tend to have lower location precisions. Therefore, they are unusable for location tracking indoors and collecting mobility data for larger crowds in smaller areas like airports, shopping centers, etc. In order to come up with a solution to this problem, networking companies like Cisco, are coming up with new location tracking technologies making use of the user connectivity to the wireless Access Points (APs) rather than relying on the satellites. These technologies extending the wireless infrastructure to provide a highly accurate location information of the Wi-Fi connected clients are being referred to as the Hyperlocation solution. While the traditional location based services used lateration, Hyperlocation uses Angle of Arrival to deliver precise location information; hence, calling for elevated developments in the Angle of Arrival estimation methodologies.

1.2 Purpose

A rising demand in the area of user mobility analytics has led to an increase in the research and development of direction finding systems for the Hyperlocation solution. Today, there are numerous studies and available technologies which offer different types of methods used for indoor location based services. Each of these methods have their pros and cons; and provide different levels of accuracy for different deployment scenarios. The most widely used direction finding methods are:

1.2.1 Cell of Origin

By making use of the Access Point that the user device is connected to, an assumption is made as to where the device is located according to that Radio Frequency (RF) cell area. While determining the location of a device using cell of origin, no distance estimation is performed. However, cell of origin technique is extremely reliant upon the client device making a smart decision during association or roaming. If the device chooses to associate to an Access Point on the floor above/below or in a completely different area because it has the strongest received signal strength, the location accuracy is lost [23].

1.2.2 Distance Based (Lateration) Techniques

The distance based techniques are typically summarized into two different methods: time based and Received Signal Strength Indicator (RSSI) based.

- Time based lateration: In the time based method, the device sends a signal with an exact start time. This signal is then picked up by multiple receivers using the start time to determine the distance from transmitter to receiver. Thus, for the time based method, it becomes crucial that all devices synchronize with a common clock source.
- RSSI lateration: RSSI lateration doesnt require the use of any synchronized clocks or relative time measurements. For this method, at each receiver that detects the signal generated by the device, the distance is measured based on the strength the signal was received at. Thus, a well thought out design is required for RSSI lateration as it is highly dependent on the degree of obstruction (or clutter) present in the environment, which can attenuate the signal.

1.2.3 Angle-Based (Angulation) or Angle of Arrival (AoA) Techniques

The angle of arrival based techniques measure the location of the client device by calculating the angle of incidence at which the signals arrive at the receiver. For this location methodology to work, at least two receiving sensors are required. Most common techniques tend to use an array of receiving elements to sample the signal in a single placement point, eliminating the need for complex antenna systems [23]. This technique suffers from decreased accuracy and precision when confronted with signal reflections from surrounding objects.

Considering the cons and pros of the various techniques, it can be observed that the angle of arrival approach has the least dependent factors and is only limited by the background signal reflections. This limitation can be easily overcome by using multiple modules in the form of Access Points to calculate angle of arrival of a client device and then combining the results. However, due to the presence of multiple antennas, angle of arrival systems can become highly computationally expensive, thus slowing down the direction finding process.

1.3 Problem Statement

The Hyperlocation solution pertaining to the angle of arrival technique is preferred over the other location techniques as it offers the least limitations and easily melds into the existing wireless Access Point infrastructure, thus, avoiding the need for deploying additional hardware. There are many algorithms being proposed for calculating the angle of arrival, based on a given scenario. Most common of them are Capon's algorithm, Bartlett's method, Multiple Signal Classification (MUSIC) algorithm, and correlative interferometry. Out of the aforementioned methods, correlative interferometry is currently the most widely used technique in the wireless industry, and will be the focus of this thesis.

The correlative interferometry based angle of arrival estimation method is based on digital beamforming and tends to dwell on the use of multiple antennas in an antenna array. This, in turn, increases the complexity of the algorithm by increasing factors like search resolution for vector correlation, long lookup times for isolating maximum angle of arrival values, etc. These factors lead to latency in the runtime on weaker processors, and increased traffic queues if the algorithm is being run on a central cloud. Hence, this thesis provides an in-depth look into the approach of correlative interferometry and

suggests amendments to the existing technique by presenting methods to reduce search resolution for correlation computations, and using interpolation or curve fitting for faster lookups. The thesis then compares the accuracy results of the suggested approach with the current approach being used in the industry and also provides a runtime comparison of the algorithm on various hardware platforms.

1.4 Thesis Organization

There are 6 chapters in this thesis. The subsequent chapters are as follows:

Chapter 2 details the necessary background information on different elements of a typical direction finding system. It gives an overview of direction finding and its application in the modern world. Basic direction finding terminology like bearings, azimuth angle, elevation angle are outlined. This is followed by an introduction to general signal processing methods like angle of arrival, time difference of arrival, received signal strength, and amplitude comparison.

Chapter 3 presents a summary of existing research work in the field of direction finding. It gives a brief overview of different algorithms and techniques used to attain angle of arrival estimation.

Chapter 4 initially explains the digital beamforming concept and its application on various antenna arrays. This is then followed by a detailed discussion of correlative interferometry and angle of arrival estimation algorithms currently being used in the industry. Afterwards, the proposed solution to reduce the computation complexity is listed by breaking it down into various methods to achieve the desired result.

Chapter 5 gives the accuracy comparison of the proposed method with respect to the original. It also discusses the runtime comparison between both the algorithm on various hardware platforms.

Finally, Chapter 6 summarizes the overall results and future work is proposed.

Chapter 2

Background

This section describes the necessary background information relevant for the work done in this thesis. The initial sections give an introduction about direction finding and its applications in the real world. Subsequent to it, the basic parameters of direction finding like bearings, azimuth angle and elevation are discussed. It is followed by a description of basic direction finding techniques such as Angle of Arrival, Time Difference of Arrival, and Amplitude Comparison.

2.1 Direction Finding

2.1.1 Overview

Direction Finding (DF), also known as Radio direction finding (RDF), refers to the use of specialized instruments, antennas, and methodologies to determine the physical location of a source from which a received signal was transmitted. This can refer to radio or other forms of wireless communication. By combining the direction information from two or more suitably spaced receivers (or a single mobile receiver), the source of a transmission may be located in space via triangulation [19]. Triangulation is the process of determining the position of an unknown node by using the angular calculation from known beacon positions. The localization of the source is a complex process and hence, done in multiple stages.

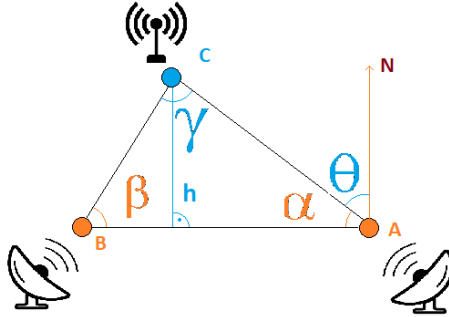


Figure 2.1: Triangulation scheme.

Generally, direction finding is intended for distant targets with the accuracy and range varying with the application and technique used. Targets may be moving or stationary. This thesis will focus on stationary targets. In order to locate the direction of a specific source, the Direction-Finding techniques look at possible sources of variation in the received signal. Possible areas of these variations are signal amplitude, signal frequency, and signal phase. Usually, only one out of these variation sources is used by a given direction finding technique.

A typical direction finding system consists of:

- DF antenna - Design varies with methodology and application.
- Receivers - Generally one or more receiver channels are present. They are used to carry out the analog-to-digital conversion of the received signal.
- Processing Unit - Digital Signal Processing unit is used to carry out the Direction-Finding algorithms based on the received data.
- Display and Control - Used to display/map the calculated location of the source by the DF algorithms.



Figure 2.2: Flow of information in direction finding system.

2.1.2 Applications of direction finding

Previously, the most common use of direction finding was for navigation purposes. However, after the introduction of satellite navigation systems, direction finding is finding its applications in determining the location of mobile targets within short distances.

Today, most common applications of direction finding include:

- Hyperlocation - Developed by Cisco Systems, hyperlocation delivers unprecedented 1- to 3-meter Wi-Fi client location accuracy. The same business and personal benefits that GPS and mobile map services have brought to the outdoors are now being realized in the indoor enterprise space, including wayfinding in malls, hospitals, airports, etc. [22]
- Radiomonitoring - Direction finders detect any signal from 300 kHz to 8.2 GHz in practically no time. They are being used to search for sources of interference, location of unauthorized transmitters, etc. Radiomonitoring mainly uses two or more measurements of the same signal, and then uses slight differences between the measurements to determine the direction of the source. This is used in surveillance for security purposes.
- Military - Direction finding techniques form a key component of military signal intelligence systems. They are used in detecting activities of potential enemies and gaining information from enemy communications.
- Research - Radioastronomy, Earth remote sensing, etc. are some of the many applications of direction finding in the area of scientific research.

2.1.3 Passive direction finding

At present, most advanced passive direction finding systems, for instance, the Cisco Hyperlocation module, tend to only work on the received signals from external sources. They

do not transmit or produce signals of their own. These systems do not have any prior knowledge of the properties of the received signal during transmission to determine the target's distance or speed.

Despite of this major limitation, the passive direction finding systems are more valuable than the conventional radar based direction finding systems. Since the passive direction finding systems lack a transmitter, their power requirement is considerably low. Lack of a transmitter also helps in concealing their location to other receivers.

These systems are able to determine the target location, direction of emitters, and type of emitters by analyzing the received signal. They are primarily designed around determining the characteristics of the incoming signal. The most common characteristic used today is the Angle of Arrival (AoA). There are many methods deployed for determining the Angle of Arrival of an incoming signal, which include: time difference of arrival (TDOA), amplitude comparison, and phase interferometry. All three of these methods require a minimum of two antennas [21]. This thesis will primarily focus on phase interferometry as it directly operates on the antenna radiation pattern, which will be discussed further in chapter 4.

2.2 Bearings

2.2.1 Overview

Lines of Bearings (LOB) or simply Bearings are generated by direction finding systems. Bearings generally indicate a direction, usually towards the target signal. This measurement is relative to the current position of the direction finding system, generating the bearing. The line of direction is indicated by the horizontal angle between the line and a defined reference line (called meridian) and at times accompanied by quadrant letters (e.g. N30°E). Bearings are given in degrees or radians.

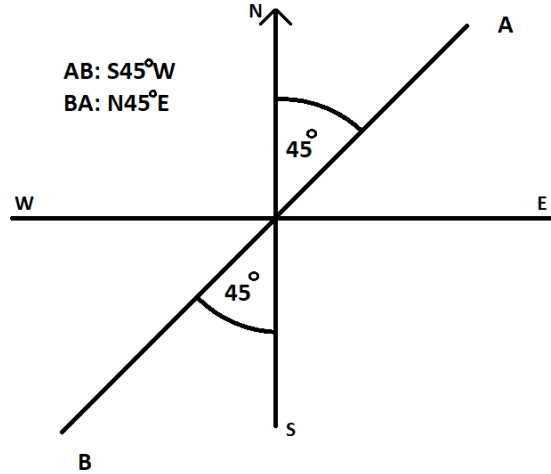


Figure 2.3: Bearings depicted by lines AB and BA in the south-west and north-east direction.

Direction finding systems use multiple bearings obtained from different sources. In order to compute the most probable location of a given target, both the bearing and the location from which the bearing was obtained should be known. When homing towards a target, only a single bearing can be used as only direction of travel is needed. The accuracy of the computed target location is directly proportional to the accuracy of the bearings, which in turn depends on the methodology used to produce the bearings. Thus, the direction finding algorithms used to compute the bearing angles and the target location tend to focus on the accuracy of the bearings.

2.2.2 Angle of Arrival

Angle of Arrival is defined as the angle that the propagation direction of the incident wave makes with some reference plane, when it arrives at the antenna array. The reference plane generally has a fixed direction against which the Angle of Arrivals are measured. The unit of measurement can be degrees or radians. Occasionally, Angle of Arrival is also commonly termed as the Direction of Arrival (DoA). In some cases, in order to determine whether a signal is arriving at an antenna, the power of the incident signal is measured, leading to a loose translation of Angle of Arrival as Power of Arrival (PoA). In direction finding systems, Angle of Arrival is the most commonly used bearing.

Angle of Arrival is usually measured in terms of Azimuth and Elevation angles, based on a spherical co-ordinate space. To calculate the azimuth angle, the vector from the origin to a given point is projected perpendicularly on a reference plane (x,y plane). The angle measured between the projected and the reference vector, on the reference plane, is called the Azimuth. Azimuth angle ranges from 0 to 360 degrees. For a point (x,y,z) in the Cartesian coordinate with respect to the origin, the corresponding azimuth angle is given by:

$$\theta = \arctan \frac{|y|}{|x|} \quad (2.1)$$

The values of θ in equation 2.1 lie in the range of 0-90°. To find the actual azimuth angle, the quadrant in which θ lies must be determined by referring to the original Cartesian coordinate system. Based on the quadrant, the real azimuth angle can found as:

- For θ in first quadrant:
Azimuth = θ
- For θ in second quadrant:
Azimuth = $\pi - \theta$
- For θ in third quadrant:
Azimuth = $\pi + \theta$
- For θ in fourth quadrant:
Azimuth = $2\pi - \theta$

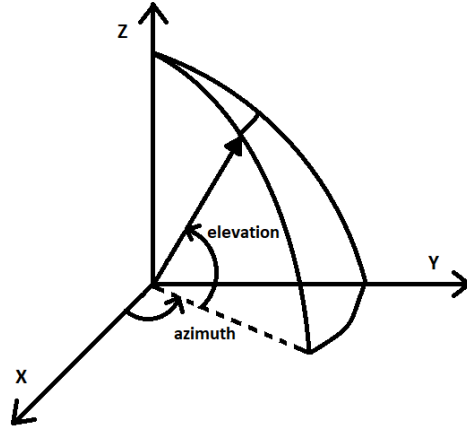


Figure 2.4: Azimuth and Elevation angles.

For Elevation, the vector from the origin to a given point is again projected perpendicularly on the reference plane. The angle then measured between the projected and the reference vector, on the vertical plane (plane containing the reference vector and the z-axis), is called the Elevation angle. Elevation angle ranges from -90 to 90 degrees. For this thesis Elevation angle will remain between 0 to 90 degrees, due to direction finding being done by a ceiling mounted Wi-Fi access point. For a point (x,y,z) in the Cartesian coordinate with respect to the origin, the corresponding elevation angle is given by:

$$\phi = \arctan \frac{\sqrt{x^2+y^2}}{z} \quad (2.2)$$

Antennas used to measure Angle of Arrival are typically closed loop arrays of multiple directional antennas. The number of antennas varies from four antennas to thirty-two antennas depending on the required location estimation accuracy.



Figure 2.5: CISCO's HALO Antenna[22].

Figure 2.5 shows CISCO's HALO Antenna module, depicting a closed loop array of thirty-two planar antennas. The increased number of antennas allows the module to not only receive the Received Signal Strength Intensity (RSSI) of the client to calculate its distance, but also analyzes the difference in timing to work out the direction of the client. In this case, the Angle of Arrival provides the direction of the client and the RSSI provides the distance.

2.3 Time Difference of Arrival (TDoA)

The Time Difference of Arrival is a popular approach for determining the Angle of Arrival using two or more antennas, positioned with a known geometry. Due to the difference in the paths between the transmitter and the receiving antennas, there is a difference in arrival time of the signal at each antenna. These time differences are represented as hyperbolae, and their intersection gives us the location of interest thus giving the Time Difference of Arrival approach the name Hyperbolic direction finding.

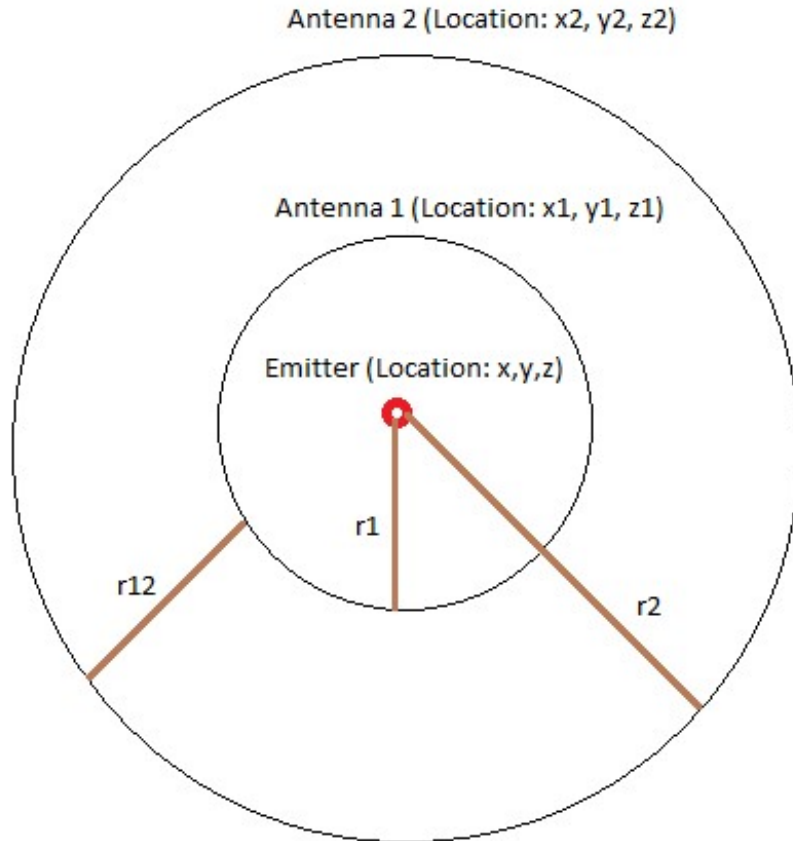


Figure 2.6: Two-antenna system.

Figure 2.6 shows a two-antenna system with an emitter at the center. The location of the Antenna 1 is given by Cartesian co-ordinates x_1, y_1 , and z_1 ; and for Antenna 2 as x_2, y_2 , and z_2 . There is an emitter located at the position given by the co-ordinates x, y , and z . The antennas, Antenna 1 and Antenna 2 are distance r_1 and r_2 away from the emitter. Each antenna sits on one of two concentric circles centered on the emitter. The radial distance between these circles is given by r_{12} . The distance of the emitter to the Antennas can be simply calculated by the distance formula as:

$$r_1 = \sqrt{(x_1 - x)^2 + (y_1 - y)^2 + (z_1 - z)^2} \quad (2.3)$$

$$r_2 = \sqrt{(x_2 - x)^2 + (y_2 - y)^2 + (z_2 - z)^2} \quad (2.4)$$

Taking the speed of the transmitted wave as c m/s in the given atmosphere, Time of Arrival at the Antennas can be calculated as:

$$t_1 = \frac{\sqrt{r_1}}{c} \quad (2.5)$$

$$t_2 = \frac{\sqrt{r_2}}{c} \quad (2.6)$$

In practical scenarios, r_1, r_2, t_1, t_2 are unknown. However, measuring the time difference of arrival between the signals at both the antennas as $t_2 - t_1$ allows the system to calculate the difference in radial distance from the emitter to each antenna $r_{12} = r_2 - r_1$. Combining the above equations gives:

$$\sqrt{(x_1 - x)^2 + (y_1 - y)^2 + (z_1 - z)^2} = \sqrt{(x_2 - x)^2 + (y_2 - y)^2 + (z_2 - z)^2} + r_{12} \quad (2.7)$$

Squaring the equation 2.7 gives us the equation of a hyperboloid. The emitter lies on this hyperboloid at some point (x, y, z) [6]. When two or more antennas are used in a similar system, the time differences can be seen as hyperbolae which cross at the location of the emitter. Increasing the number of antennas adds additional constraints on the possible location of the emitter on the curve, thereby, further increasing the accuracy.

The Time Difference of Arrival technique of direction finding tends to be very precise and yields the location of the target along with its direction. However, to achieve high time of arrival accuracy in the time measurement, which in turn determines the accuracy of the Angle of Arrival, the antennas need to be placed a distance on the order of kilometers apart. Therefore, Time Difference of Arrival falls short in small-scale systems where distances are smaller and high precision is required.

2.4 Received Signal Strength Indicator (RSSI)

In direction finding, the Angle of Arrival, the time of arrival, or the received power of the signal at the antenna, also known as the Received Signal Strength Indicator (RSSI), are used for target localization. RSSI has no absolute value. It is primarily a term used to measure the relative quality of a received signal to a client device. There are many

different approaches to measure the Angle of Arrival. Out of these, the most popular methods are using the antenna array with known array geometry, and then measuring of different signal arrival times at different antennas. This approach is basically Time Difference of Arrival (TDoA). The second approach to estimate the Angle of Arrival is to use the RSSI ratio between two or more directional antennas on the sensor node. Most researchers use directional rotatable antennas and measure the peak power of the received signal. Most modern radio modules support the RSSI, which helps measure the received power for each received packet at the antenna. The power or energy of a signal travelling between two nodes (transmitting and receiving) is a signal parameter which can be used for distance estimation [14].

2.5 Amplitude Comparison

Another primary technique for determining Angle of Arrival is the Amplitude Comparison method. The amplitude comparison method measures the difference in amplitudes received from two or more directional antennas whose boresights are pointed in different directions. Generally, the number of antenna elements is reduced to two, as a wide beam is required in this method. The amplitude comparison between two adjacent antennae gives the largest and next to the largest amplitude to provide the Angle of Arrival of the received signal.

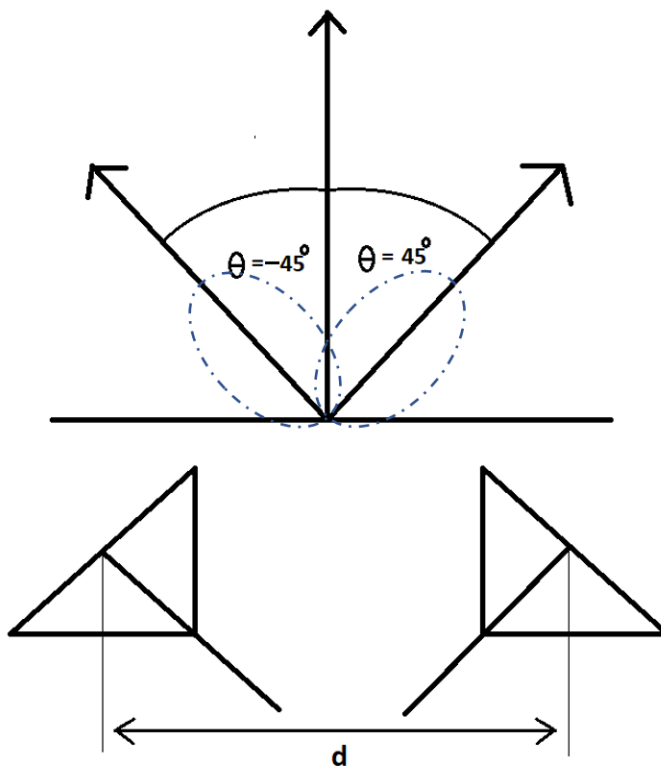


Figure 2.7: Two antenna with boresights offset by 90 degrees.

When a signal arrives, the amplitude-comparison receiver compares the ratio of power amplitudes between the two antennas to some pre-recorded antenna gain patterns. This is in turn used to calculate the Angle of Arrival. The Angle of Arrival can be determined to one of the pre-recorded values due to the power ratios being compared to known values. The effectiveness of this method is directly affected by the amount of memory dedicated to store the known values [21]. Amplitude comparison is one of the most common techniques being low cost by using low resolutions. However, it suffers from poor accuracy and sensitivity due to the use of broad-beam antennas.

Chapter 3

Literature Review

At present, most of the Direction Finding (DF) systems yield bearings to determine the direction. The most common type of these bearings are termed as Angle of Arrival (AoA). Angle of Arrival, being a broad term, generally means the measure of the angle(s) at which a signal arrives at an antenna array. In order to detect if a signal is arriving at an antenna, the power of the incoming signal at one or more antennas is determined. A common way is to take the phase or the time differences of the arriving signal at different elements as a measure for Angle of Arrival. The following chapter is aimed at discussing different methodologies carried out by researchers for Angle of Arrival measurements.

3.1 Triangulation Method - Rotating Beacons

AoA estimation using triangulation is discussed in [26]. In the paper, a cluster-based architecture where the cluster head (CH) acts as an anchor node, is used. This model proposes using the Angle of Arrival and Triangulation method to locate the position of the unknown nodes (randomly deployed) using the information from the Cluster Head and the angle which the Cluster Head makes with the unknown node. Each sensor node uses Angle of Arrival of the beacons to estimate its position.

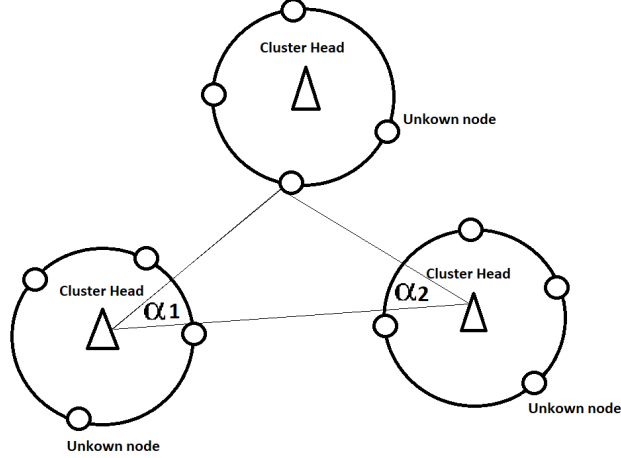


Figure 3.1: System Model.

The anchors are transmitting their beacons in turn, not simultaneously. Each beacon is started by sending the anchor position, which is followed by a strong short omni-directional beacon. Then the rotating beacon is transmitted with constant angular speed ω , which all the sensors are aware of. The sensors are trying to register the moment when the power of the beacon is the strongest. A difference in time between receiving the initial pulse and the maximum of the beacon power allows calculating the angle-of-arrival of the signal: α_i . The angle α_i (from the i -th anchor) can be used in an equation binding the coordinates of the CH and the sensor node.

$$X_i - x_i = Y_i - y_i \tan \alpha_i \quad (3.1)$$

In equation 3.1, $[X, Y]$ and $[x_i, y_i]$ are the coordinates of the sensor and the i -th anchor, respectively. If the angles of arrival from two or more anchors are known, the sensor can estimate its position using the traingulation method. When two CHs are used, the required location will be identified as the third point in a triangle of two known angles (the bearings from each reference point), and the distance between reference points, as seen in equatioin 3.2

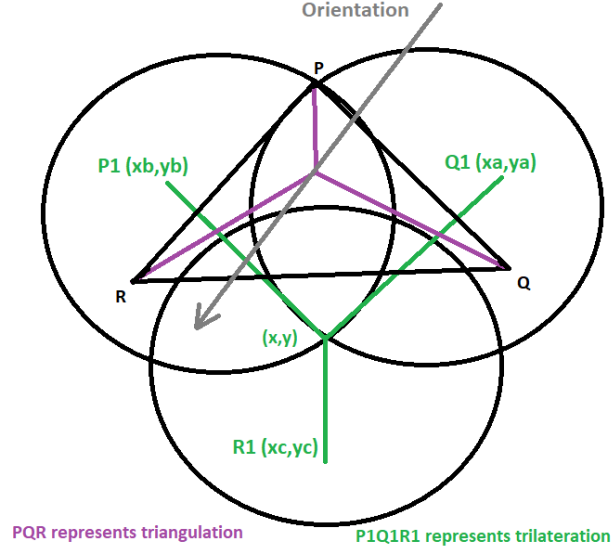


Figure 3.2: Triangulation and Trilateration

$$x = x_2 + \cos \alpha_2 \frac{y_2 - y_1 - \tan \alpha_1 (x_2 - x_1)}{\cos \alpha_2 \tan \alpha_1 - \sin \alpha_2} \quad (3.2)$$

where,

α_1 and α_2 are the known angle,

(x_1, y_1) and (x_2, y_2) are the known coordinates of the CHs,

(x, y) are the coordinates of the unknown node to be found.

It can be seen that this approach for AoA estimation relies heavily on the cluster geometry and initial conditions like the angle the CH makes with the unknown node, for more than one anchor. This is not possible in most scenarios.

3.2 Cooperative AoA Localization Scheme (CALS)

Authors in [25] present another approach to calculate AoA estimation for location processing called the Cooperative AoA Localization Scheme. This method relies on the distance information between different antenna nodes to determine the AoA; thus, making distance between two nodes a vital factor for the algorithm to function. The precision of AoA depends directly upon the accuracy of distance estimation. CALS makes use of RSSI for estimating the distance between nodes. The relation between RSSI and the distance between nodes can be written as:

$$RSSI \propto \log \frac{Pr}{Pr_{ref}} \quad (3.3)$$

$$Pr = \frac{K}{d^\alpha} \quad (3.4)$$

Here, Pr represents the power received at a distance d , K is the proportionality constant, α being the signal propagation constant, and Pr_{ref} is equal to 1mW. The above two equations yield

$$RSSI = K1 \log d + K2, \quad (3.5)$$

where $K1$ and $K2$ are constants. Thus, we obtain

$$d = 10^{\left(\frac{K2-RSSI}{K1}\right)} \quad (3.6)$$

In the equation 3.6, the authors of [25], using experiments, have approximated $K1$ and $K2$ for indoor localization scenarios. However, the approximated coefficients $K1$ and $K2$, will result into approximated distance, thus providing limited accuracy. This limited accuracy will result into limited precision of AoA estimation adding error to the localization of nodes.

3.3 Digital Beamforming Approach

Most of the current AoA estimation methods are based on the idea of digital beamforming. [20], [13], and [9] demonstrate some of these different approaches. The authors of [20] have given a general AoA estimator system scheme, which is represented in Figure 3.3 below.

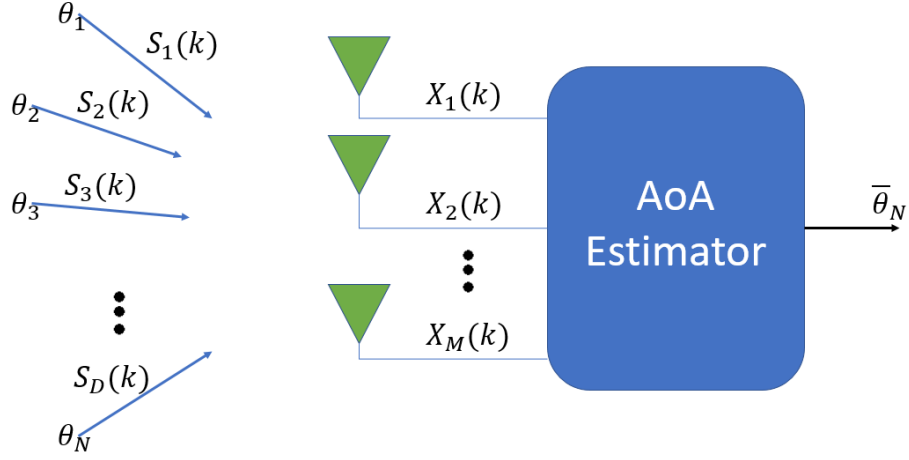


Figure 3.3: General scheme of AoA system

Figure 3.3 shows D incident signals on a linear array with M -elements from angles θ_D . The received signals $x_m(k)$ are given by,

$$\bar{x}(k) = \bar{A} \cdot \bar{s}(k) + \bar{n}(k) \quad (3.7)$$

where,

$A = [a(\theta_1)a(\theta_2)a(\theta_D)]$ is the $M \times D$ matrix of steering vectors, which represents the set of phase delays experienced by a plane wave as it reaches each element in an array;

$\bar{s} = [\bar{S}(k_1)\bar{S}(k_2)\bar{S}(k_D)]^T$ is the vector of incident signals at time k

$\bar{n}(k)$ is the $1 \times D$ noise vector at each array element M with zero mean and covariance matrix between the noise vectors $R_{nn} = \sigma^2 \bar{I}$

Furthermore, each steering vector corresponding to uniform linear array is given by,

$$a(\theta_D) = [1e^{jd \cos \theta} e^{2jd \cos \theta} \dots e^{((M-1)jd \cos \theta)}] \quad (3.8)$$

where d is the distance between array elements.

The signal of interest $x_m(k)$ contains useful information and noise, with covariance matrix given by

$$\bar{R}_{xx} = \bar{A}\bar{R}_{ss}\bar{A}^H + \bar{R}_{ss} \quad (3.9)$$

Assuming ergodicity, the matrix correlation of the incident signal \bar{R}_{xx} can be approximated as follows:

$$\bar{R}_{xx} \approx \frac{1}{K} \sum_{k=1}^K \bar{x}(k)\bar{x}^H(k) \quad (3.10)$$

The results of AoA algorithms are represented based upon maxima vs. angle through a function known as pseudospectrum. Some basic AoA algorithms are covered in subsections [3.3.1](#), [3.3.2](#), and [3.3.3](#)

3.3.1 Bartlett

The Bartlett estimation is equivalent to the rapid Fourier Transform in the spatial domain of all incident signals. It can also be interpreted as adding beam-steered array factors for each angle of arrival and finding its absolute value squared. Equation [3.11](#) is used to estimate the AoA applying Bartlett's algorithm. Some application of Bartlett application can be found in [\[18\]](#), [\[10\]](#), [\[5\]](#)

$$P_B(\theta) = \bar{a}^H(\theta)\bar{R}_{xx}\bar{a}(\theta) \quad (3.11)$$

3.3.2 Capon

This estimation is based on the widely known Minimum Variance Distortionless Response (MVDR) criterion. It is also interpreted as a Maximum Likelihood estimation of a signal arriving from one direction while the rest of the incident signals are considered as interference, hence the criterion is to maximize the Signal to Interference Ratio (SIR). It assumes that the source signals are uncorrelated. Capon has better resolution than Bartlett, however if the source signals are correlated its performance suffers from a severe degradation and in that scenario it is better to use Bartlett. Equation [3.12](#) represents Capon's equation to estimate the AoA. Some application of Capon can be found in [\[30\]](#), [\[12\]](#), [\[7\]](#)

$$P_C(\theta) = \frac{1}{\bar{a}^H(\theta)\bar{R}_{xx}^{-1}\bar{a}(\theta)} \quad (3.12)$$

3.3.3 MUSIC

MUltiple Signal Classification (MUSIC) is a very popular high resolution eigen-structure method. It provides asymptotically unbiased estimations for AoA and assumes the noise in each signal is uncorrelated. If correlation occurs its performance is severely degraded. MUSIC use equation 3.13 to the estimation. Some application of MUSIC can be found in [8], [27], [29], [24]

$$P_{MU}(\theta) = \frac{1}{|\bar{a}^H(\theta)\bar{E}_N\bar{E}_N^H\bar{a}(\theta)|} \quad (3.13)$$

In equation 3.13, E_N represents the signal noise eigen vectors.

3.4 Performance Evaluation

Currently, various direction finding algorithms are being developed. For instance, the MUltiple Signal Classification (MUSIC) algorithm, maximum likelihood estimation (MLE), Capon algorithm, and many others. Although each algorithm caters to some problem associated with direction finding, they are also accompanied by different limitations and deficiencies, with high processing load being the most common among them. With the increase in the research of different direction finding algorithms in the wireless industry, the standards for achieving a good algorithm primarily hinge on the algorithm's accuracy and speed, along with size of the runtime overhead.

For most of the algorithms, Root Mean Square Error (also called the root mean square deviation) approach is used as a method of performance evaluation. The idea behind the Root Mean Square Error is to obtain a measure of the difference between values predicted by a model and the values actually observed from the environment that is being modelled. These differences are also termed as residuals, and the Root Mean Square Error combines them into a single measurement. The Root Mean Square Error of a model performance with respect to the estimated variable X_{model} is defined as the square root of the mean squared error:

$$RMSE = \sqrt{\frac{\sum_{i=1}^n (X_{obs,i} - X_{model,i})^2}{n}} \quad (3.14)$$

where X_{obs} denotes observed values and X_{model} denotes modelled values at time/place i .

Root Mean Square Error adequately represents model performance when the error distribution is Normal or Gaussian [4]. In addition, the root mean squared error avoids the use of absolute value.

Most researchers, like in [15] [2], approaching the Angle of Arrival estimation problem using a Maximum Likelihood Estimator (MLE), have used Root Mean Square Error for performance assessment. Generally, a MATLAB computer simulation is carried out to find the angle of arrival of the target. Then the performance of the iterative MLE approach is compared using the root mean squared error method with the grid search method where a conventional coarse grid search is followed by a refined search. At each AoA value, 1,000 runs of the algorithm are performed with both the iterative MLE and the grid search method. A good indication of how well the algorithm performs can be seen by comparing its result to the predicted or expected value.

However, most numerical methods which are used to locate the maximum of the likelihood function are often based on the use of gradients. Such methods tend to locate the local maximum nearest to the initial estimation. They will perform poorly when the likelihood function has many local maxima. The AoA estimation problem falls into this category, since the likelihood function for a K-element array typically has K local maxima. To avoid this pitfall, such numerical search methods either require a priori information about the AoA or use additional computations to sample the likelihood function to get an approximate location for the global maximum [2].

Chapter 4

Digital Beamforming and Direction Finding

Beamforming is the combination of radio signals from a set of small non-directional antennas to simulate a large directional antenna. In communications, beamforming is used to point an antenna at the signal source to reduce interference and improve communication quality. In direction finding applications, beamforming can be used to determine the direction of the signal source [11]. This chapter will initially go over Antenna Radiation Patterns, Directional Antenna Arrays, and basics of Digital Beamforming. Later section 4.5, discusses techniques for direction finding using correlative interferometry. This is followed by different alterations to the algorithm in section 4.6, ultimately arriving at the proposed solution in section 4.7 The alterations are aimed to reduce the complexity of the initial algorithm mentioned in section 4.5, while maintaining the accuracy.

4.1 Antenna Radiation Patterns

For an antenna, a radiation pattern refers to a plot of field strength vs. direction of the antenna. The definition remains the same, irrespective of the type of antenna: receiving or transmitting. The radiation pattern graphically represents the antenna's radiation properties in space by depicting how an antenna is radiating energy in all three dimensions. Therefore, the antenna radiation pattern is actually three dimensional. This three-dimensional pattern is however represented using two planar patterns, called the principal plane patterns. These principal plane patterns can be obtained by making two

slices through the three-dimensional pattern through the maximum value of the pattern or by direct measurement. It is these principal plane patterns that are commonly referred to as the antenna patterns [16]. Usually, the principal planes are encountered in terms of azimuth plane and elevation plane. They are especially helpful in plotting the radiation patterns when there are multiple side lobes to be expected in the pattern. All antenna radiation patterns consist of portions called lobes. A lobe is any part of the pattern that is surrounded by regions of relatively weaker radiation [16]. Thus, lobes can be main lobe, side lobe, etc.

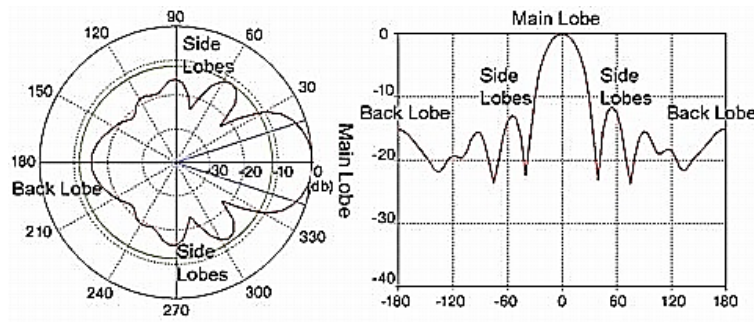


Figure 4.1: Antenna radiation pattern in Polar and Cartesian coordinates[16]

A main lobe of an antenna radiation pattern represents the lobe containing the direction of maximum radiation power. The lobes other than the main lobes are called side lobes. The angular width of the main lobe of an antenna field pattern is termed as beamwidth of an antenna. When this angular width is measured between the points on the main lobe that are 3-dB below the peak of the main lobe, it is called Half-Power BeamWidth (HPBW) or 3-dB beamwidth.

4.2 Directional Antenna Array

4.2.1 Directional Antennas

Directional antennas are antennas that are designed to focus the gain in one particular direction. The gain of an antenna is defined as the ratio of the radiation density in a particular angular direction in space to the total input power to the antenna [11]; that is,

$$G(\phi, \theta) = \frac{4\pi \text{ times the power radiated per unit solid angle in directions } \phi, \theta}{\text{Total input power to the antenna}} \quad (4.1)$$

where:

$G(\phi, \theta)$ = Gain of the antenna

ϕ = Azimuth angle

θ = Elevation angle

The size of the antenna helps in increasing the coverage distance of the antenna, however, decreasing the effective coverage angle. These antennas have better control over the antenna radiation pattern, with the main lobe pointing in the direction of propagation. The directive gain in this direction of maximum radiation density is commonly termed as the Directivity of the antenna. The maximum gain of an antenna G is simply the product of the directivity and the antenna efficiency; where the antenna efficiency is defined as the ratio of total power radiated by the antenna and the total power input to the antenna.

$$G = D\eta \tag{4.2}$$

Where:

G = Maximum gain of the antenna

D = Directivity of the antenna

η = Efficiency of the antenna

Figure 4.2 shows the antenna field pattern of a directional antenna. It has a narrow central main lobe of high gain and almost negligible gain focused on the back lobes and side lobes. The directions where signal strength is zero are called nulls.

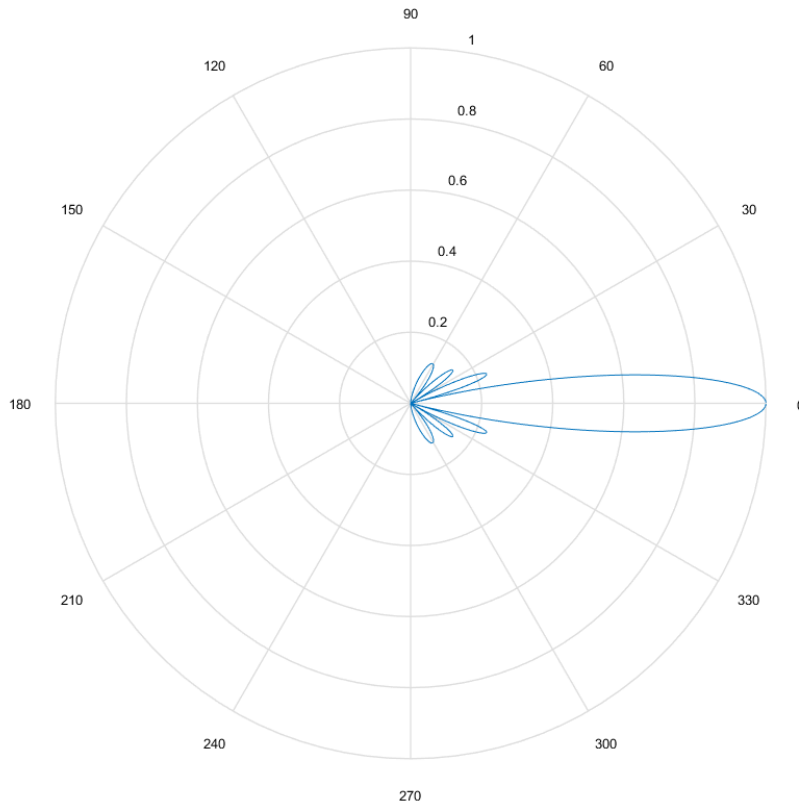


Figure 4.2: Radiation pattern of a Directional Antenna

4.2.2 Array Antennas

In most antenna applications like point-to-point communication, direction finding, a highly directive antenna beam is needed. The directive beam can be obtained by using an array of directional antennas with high gain and low side lobe levels. On increasing the directivity of an antenna, the overall gain also increases. This increase in directivity results in an antenna receiving less interference from its surroundings. The antenna arrays are also capable of steering beams in the required radiation direction. Unlike single antennas, where the radiation pattern is fixed, array antennas can vary the radiation pattern, which is called the array pattern. This ability of array antennas to change the radiation pattern is obtained by having different excitations of the antenna elements of the array. It is possible

to obtain a certain array pattern without actually changing the physical parameters of the antennas. Thus, array antennas allow for much more sophisticated tasks with signal processing like spatial filtering, gain enhancement, target tracking, etc. This thesis uses different kinds of antenna arrays, some of whose basic antenna patterns are discussed in the following sections.

4.2.3 Linear Array

The most simple implementation of an antenna array is a uniformly linearly spaced array of identical isotropic elements. Figure 4.3 shows such an array with K uniformly spaced identical elements. Each element has a complex weight of V_k with $k = 0, 1, 2, \dots, K - 1$. Complex weight is generally the combined relative amplitude and phase shift for each respective element. The interelement spacing is d . In this structure shown, a plane wave is incident on the array, making an angle θ with the array normal. Since any two ray paths have a separation of $d \sin \theta$ between them, the wavefront always arrives at element $k + 1$ sooner than the element k .

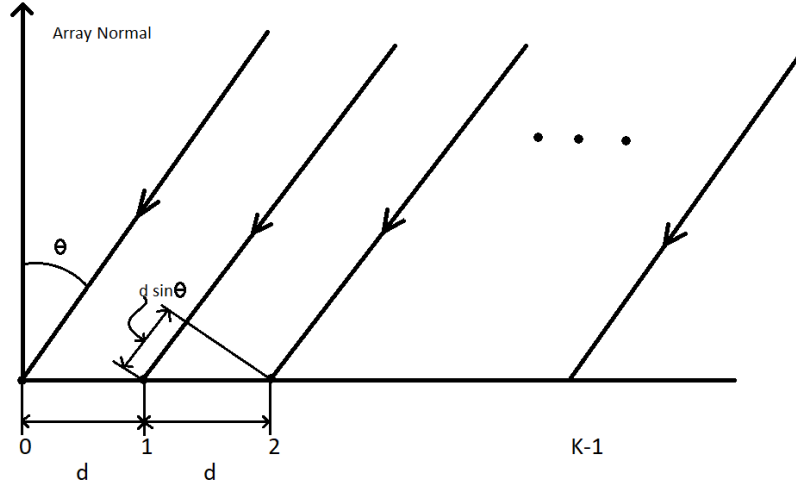


Figure 4.3: Uniformly Spaced Linear Array

If the phase of the signal incident at the element located at the origin is zero, the phase of the signal at element k relative to element 0 will be:

$$\kappa k d \sin(\theta) \tag{4.3}$$

where:

$$\begin{aligned} \kappa &= \frac{2\pi}{\lambda} \\ \lambda &= \text{wavelength} \end{aligned}$$

Adding all the elements together gives us the array factor F :

$$F(\theta) = V_0 + V_1 e^{j\kappa d \sin \theta} + V_2 e^{j2\kappa d \sin \theta} + \dots = \sum_{k=0}^{K-1} V_k e^{j\kappa k d \sin \theta} \tag{4.4}$$

The above equation can be re-written in terms of vector product:

$$F(\theta) = V^T v \quad (4.5)$$

where

$$V = [V_0, V_1, \dots, V_{K-1}]^T \quad (4.6)$$

is the weighing vector and

$$v = [1e^{j\kappa d \sin \theta}, e^{j2\kappa d \sin \theta}, \dots, e^{j(K-1)\kappa d \sin \theta}]^T \quad (4.7)$$

is the array propagation vector or the steering vector which gives the Angle of Arrival of the signal. The complex weight is

$$V_k = A_k e^{jka} \quad (4.8)$$

where $a =$ phase of the k th element. Thus, the array factor becomes:

$$F(\theta) = \sum_{k=0}^{K-1} A_k e^{j(k\kappa d \sin \theta + ka)} \quad (4.9)$$

If $a = -\kappa d \sin \theta_0$, the maximum response of $F(\theta)$ will result at the angle θ_0 ; that is, the antenna radiation pattern will be steered towards the signal source [11]. On increasing the total width of the array, the main lobe becomes narrower and the side lobes becomes smaller. An example of an eight element array pattern is shown below:

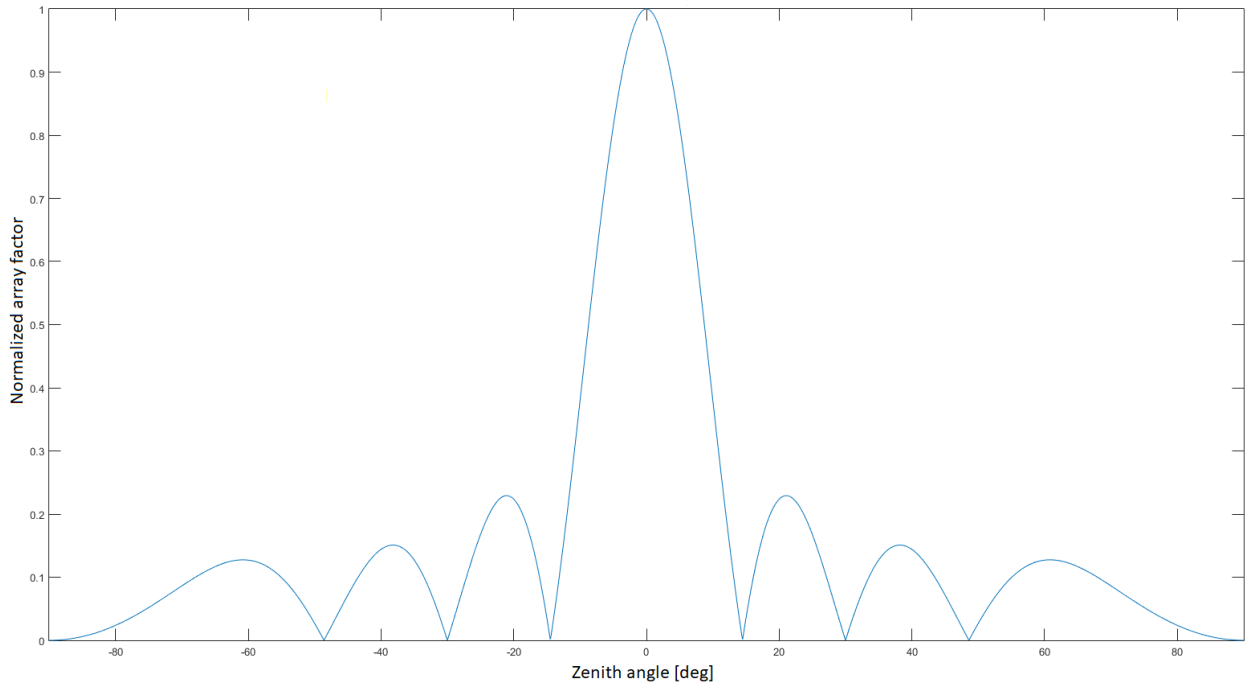
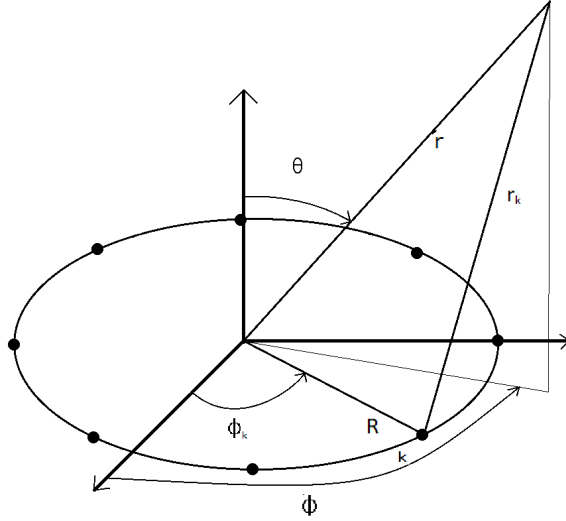


Figure 4.4: Eight element linear array pattern

4.2.4 Circular Array

Similar to linear array, an arrangement of K evenly spaced isotropic elements in a circular array is shown in Figure 4.5. The radius of the circular array is R , and each element has a complex weight V_k with $k = 0, 1, 2, \dots, K - 1$.



F

Figure 4.5: Circular Antenna Array

All the elements are equally spaced; therefore, the azimuth angle of the K th element can be given by:

$$\phi_k = \frac{2\pi k}{K} \quad (4.10)$$

For a wave incident on the antenna array in the direction (θ, ϕ) , as shown in Figure 4.5, the relative phase at the k th element with respect to the centre of the circle is given by:

$$\beta_k = -\kappa R \cos \phi - \phi_k \sin \theta \quad (4.11)$$

From similar principles, as a linear array, we can find the array factor for a circular array as:

$$F(\phi, \theta) = \sum_{k=0}^{K-1} A_k e^{j(\alpha_k - \beta_k)} \quad (4.12)$$

where:

$A_k e^{j\alpha_k}$ = Complex weight for the k th element

α_k = phase weight for the k th element, generally chosen to be $\kappa R \cos(\phi_0 - \phi_k) \sin \theta_0$

The array pattern for a circular array is shown in Figure 4.6

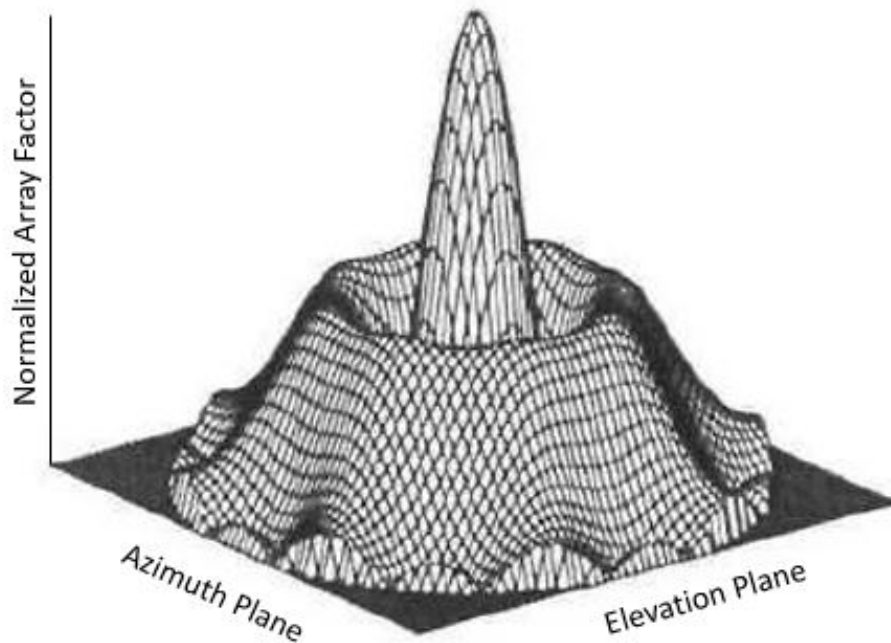


Figure 4.6: Circular array pattern[11].

4.3 Digital Beamforming

Digital beamforming involves capturing the RF signals in the form of a digital stream at the antenna level. The digital signals include the details about the amplitude and phase of the signals received at each element of the antenna array. The beamforming is then carried out by weighing the digital signals, adjusting their corresponding amplitudes and phases to obtain the required antenna radiation pattern. This technique conserves the total information available at the antenna aperture, contrary to analog beamformers, where only the weighted sum of the signals is produced and the signal dimensionality is reduced from K to 1.

The digitized signals in digital beamforming are always converted into two streams of binary basebands: I and Q signals. I represents the amplitude of the signal and Q

represents the phase. Together, the I and Q parts are used to represent the signal as a complex vector (phasor) with real and imaginary parts. The signal at time t is represented as:

$$x(t) = I(t) + jQ(t) \quad (4.13)$$

where:

$x(t)$ = complex baseband signal

$I(t)$ = is the real part

$Q(t)$ = is the imaginary part

$j = \sqrt{-1}$

This signal can be further represented in terms of an array factor as

$$F(\theta) = \sum_{k=0}^{K-1} w_k^* x_k(t) \quad (4.14)$$

where:

$F(\theta)$ = output of the beamformer

w_k^* = complex conjugate for weights for the forming beam at angle θ

x_k = signal from the k th array element

The vector $x(t)$ is commonly known as an antenna phase vector or steering vector

4.4 Correlative Interferometry

The interferometry technique was first introduced in radio astronomy [3]. It was aimed at increasing the resolution and the sensitivity of the direction finding system by superimposing the signals of antenna elements that were spaced many wavelengths apart.

The bearing calculations performed by Interferometers are based on phase differences of the signal received at multiple antenna elements. The basic principle of a correlative interferometer is to equate the measured phase differences or the measured phase vector with respect to the reference phase difference, also called the reference phase vector or ideal phase vector, obtained for a direction finding system of a given configuration at each

wave angle. The comparison involves calculating the quadratic error or the correlation coefficient of the two phase vectors. The bearing for which the correlation coefficient is at a maximum corresponds to the angle of arrival of the incoming signal.

Figure 4.7 shows a sample of reference vectors obtained for some antenna array. Each column of the matrix represents a reference vector corresponding to a certain wave angle θ . The elements of the column represent the expected phase difference between the antenna elements for that wave angle. The upper column represents the measured vector. Using these, a correlation matrix is obtained by correlating each of the reference vectors, represented by the columns, with respect to the measured vector matrix. This process results in a correlation function, whose maximum value corresponds to the azimuth and elevation angle values of the desired angle of arrival. The equation for the correlation function can be given as:

$$\rho = \frac{|V_m \cdot V_i^T|}{\sqrt{[V_m^T \cdot V_m][V_i^T \cdot V_i]}} \quad (4.15)$$

where:

ρ = Correlation value between the measured and ideal phase vectors

V_m = Measured phase vector

V_i = Ideal phase vector

If the two vectors are similar, then the correlation value is closer to 1. If the two vectors are perpendicular then the correlation value is 0; and if they are parallel and in opposite directions, then the correlation value is -1 .

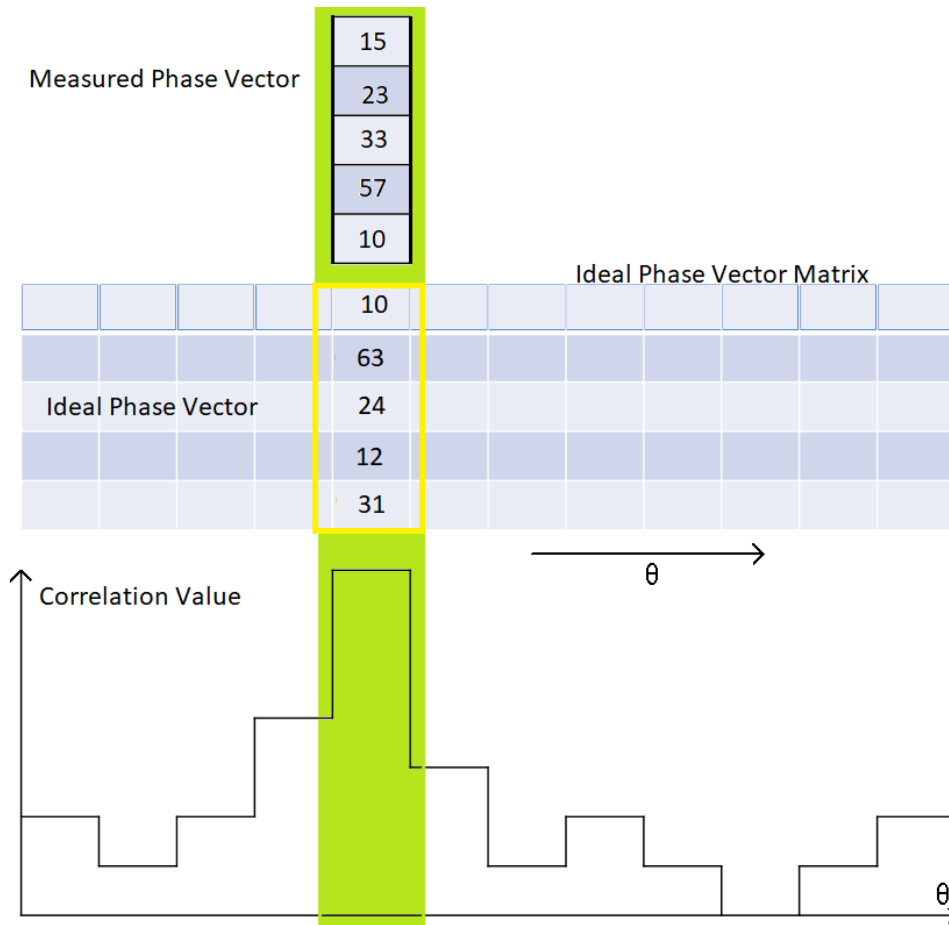


Figure 4.7: Correlation matrix and correlation function.

4.5 Direction finding Algorithm using Planar sweep

An antenna array with a known position and geometry is used in this section. For illustrations, the HALO antenna array geometry is used, shown in Figure 2.5. The antenna array is assumed to be lying in the XY Plane. The centre of the antenna array is located at a height of 10 feet from the origin. The frequency of the antenna elements is kept at the standard value of that of a router antenna, that is, 5.18 Giga Hertz. The radio waves are assumed to be moving at a speed of 300,000 km per second.

The direction finding Algorithm uses the principles of correlative interferometry to find

the value Angle of Arrival for a given target. Inputs to the algorithm consist of the antenna geometry and a test location. Based on these inputs, the value for the measured phase vector is calculated. For the reference phase vector or the ideal phase vector, phase vectors are picked by sweeping an area of fixed resolution in cartesian coordinate space to cover the three-dimensional space around the test location.

4.5.1 Obtaining the measured phase vector

To obtain the measured vectors, first, the vectors are calculated for each of the antenna array elements with respect to the given test location:

$$w_k = |A_k - l| \tag{4.16}$$

where:

$$k = 0, 1, 2, \dots, K$$

K = Total number of antenna elements

w_k = weight of vector from antenna element to the test location

A_k = Vector representing an antenna element

l = test location

Now, the weights obtained are normalized with respect to weight of a specific antenna element:

$$v_k = w_k - w_0 \tag{4.17}$$

where,

v_k = normalized weights with respect to antenna $k = 0$

Here, the test location and antenna vectors have measurement in feet, so to obtain a phasor, they have to be converted into degrees. To achieve this, the weights are first converted into meters, and then divided by the wavelength of the Radio waves. The wavelength can be obtained by utilizing the speed and frequency of the waves used.

$$v_k = v_k * 0.3048 \text{ meters}$$

$$f = 5180 * 10^6 \text{ Hz, frequency of the antenna elements}$$

$$c = 300,000,000 \text{ meters/second, approximate speed of the radio waves}$$

$$\lambda = \frac{c}{f} = 0.0579 \text{ meters}$$

$$v_k = v_k * \frac{\lambda}{360} \text{ degrees}$$

Now, the simulated measured (no noise) phase vector can be written as:

$$V_m = [1e^{(jv_1 \frac{\pi}{180})}, e^{(jv_2 \frac{\pi}{180})}, \dots, e^{(jv_K \frac{\pi}{180})}] \quad (4.18)$$

where

$$V_m = \text{Measured phase vector}$$

4.5.2 Calculating ideal phase vector

In order to obtain the maximum value of correlation for the azimuth and elevation values, the ideal phase vectors are calculated separately using an azimuth sweep and an elevation sweep. Both sweeps are done using a fixed resolution of 200x200 points for this thesis as this resolution yields the result in the desired percentage error range. For azimuth sweep, the resolution consists of the points on a plane through the test point, parallel to the plane of the antenna array. This can be seen in Figure 4.8.

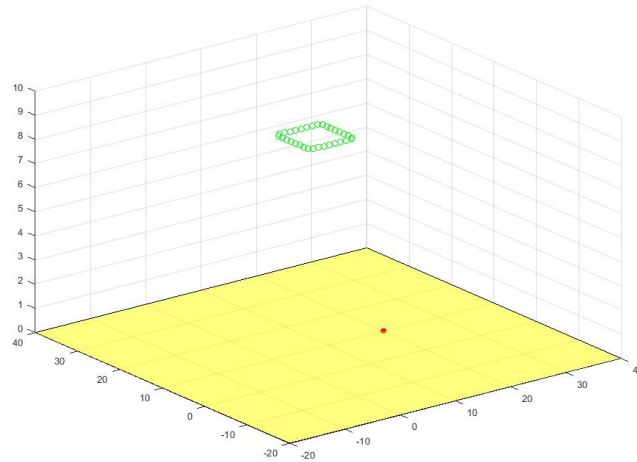


Figure 4.8: Azimuth sweep.

For every point on the resolution of the said plane, the ideal phase vector is calculated and a correlation is obtained. The operation to obtain an ideal vector for any point is similar to the process done in the calculations of the measured vector.

$$w_k = |A_k - x| \quad (4.19)$$

$k = 0, 1, 2, \dots, K$

K = Total number of antenna elements

w_k = weighted vector from antenna element to the test location

A_k = Vector representing the position of antenna element

x = Point on the resolution plane

Now, the weights obtained are normalized with respect to weight of a specific antenna element:

where,

v_k = normalized weights with respect to antenna $k = 0$

The ideal phase vector can be written as:

$$V_i = [1e^{(jv_1 \frac{\pi}{180})}, e^{(jv_2 \frac{\pi}{180})}, \dots e^{(jv_K \frac{\pi}{180})}] \quad (4.20)$$

To obtain the elevation sweep, the same procedure is repeated with the resolution consisting of the points on a plane through the test point, perpendicular to the plane of the antenna array. This can be seen in Figure 4.9 below.

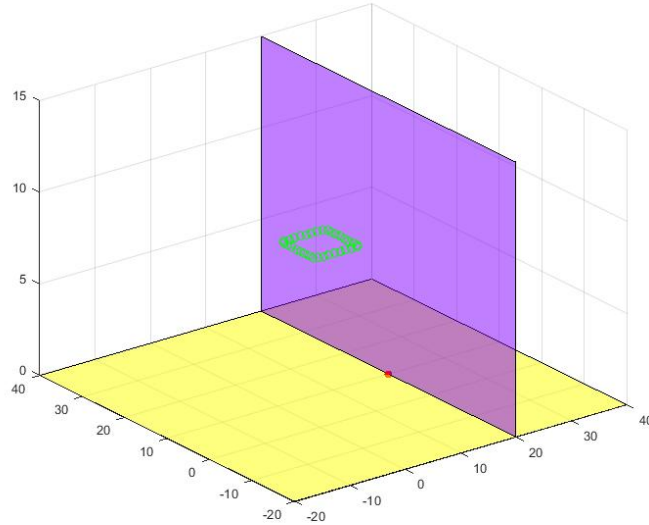


Figure 4.9: Azimuth and Elevation Sweep

4.5.3 Calculating the Correlation Matrix

After obtaining the phase vectors, the correlation matrix is obtained by taking the correlation between the measured phase vector with respect to each of the ideal phase vectors for the Azimuth and Elevation sweep. The equation for the correlation function is given by [4.15](#)

The highest values in the correlation matrix for azimuth and elevation sweep correspond to the required points with required azimuth and elevation values.

4.6 Direction finding Algorithm Using Spherical Sweep

In the planar sweep technique, the resolution used only corresponds to the azimuth and elevation planes. This makes it very limited and eventually as the target moves farther away, it fails to cover the entire space around the test point. To solve this issue, a spherical coordinate system is used for the resolution.

This method selects the sweep resolution based on a spherical surface area around the test point. The resolution used is always in a form of a hemi-sphere as the test point is

always above or below the plane of the antenna array. Figure 4.10 shows the hemi-spherical resolution around the test point for a HALO antenna.

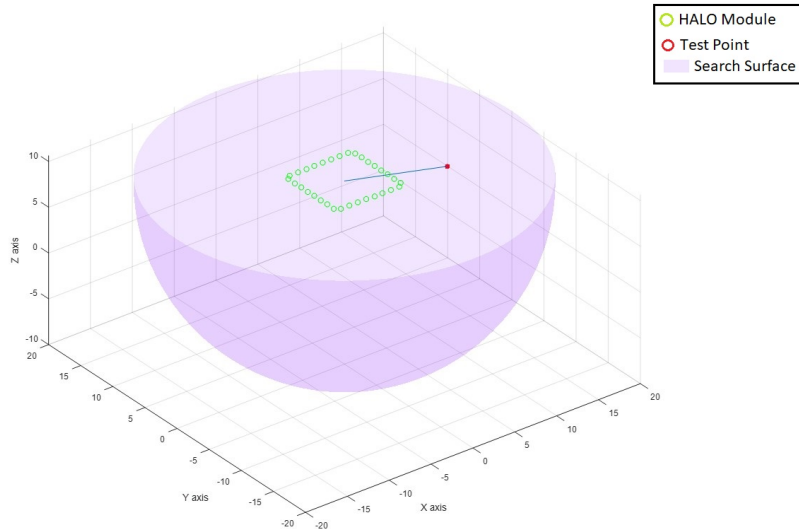


Figure 4.10: Hemi-spherical sweep.

The spherical sweep allows us to capture the entire 3D antenna radiation pattern in contrast to the planar sweep, which operates on a limited region of azimuth and elevation planes. Thus, using spherical sweep we only go through the selected resolution once, rather than using two different resolution sweeps. The calculations for the ideal phase vectors remain the same as with planar search, and the correlation matrix is obtained in a similar way.

4.7 Refining Results

4.7.1 Coarse Search and Fine Search

In both the direction finding methods, the search resolution is spread out on a bigger space. This impacts the accuracy of the final result as the key points for maximum correlation value could be missed out. One solution to extract the most accurate values for the

azimuth and elevation angle is to increase the number of points in the search resolution space. However, an increase in points over the same resolution space further adds to the computational run time of the algorithm, and is overall not efficient.

In order to achieve a better accuracy while maintaining the computational time, a better approach will be to do a coarse search on the entire resolution space, followed by a much more granular search in a restricted space. For the coarse search, the resolution is restricted to a maximum of 50x50 points. This decrease in the resolution on the same space leads to a wider separation between the points. The smaller resolution is also computationally faster and less expensive. From the result of the coarse search, based on the point corresponding to the maximum azimuth and elevation value, we select a space using points slightly below this maximum value to be used for fine search. Figure 4.11 shows a correlation plot for coarse search.

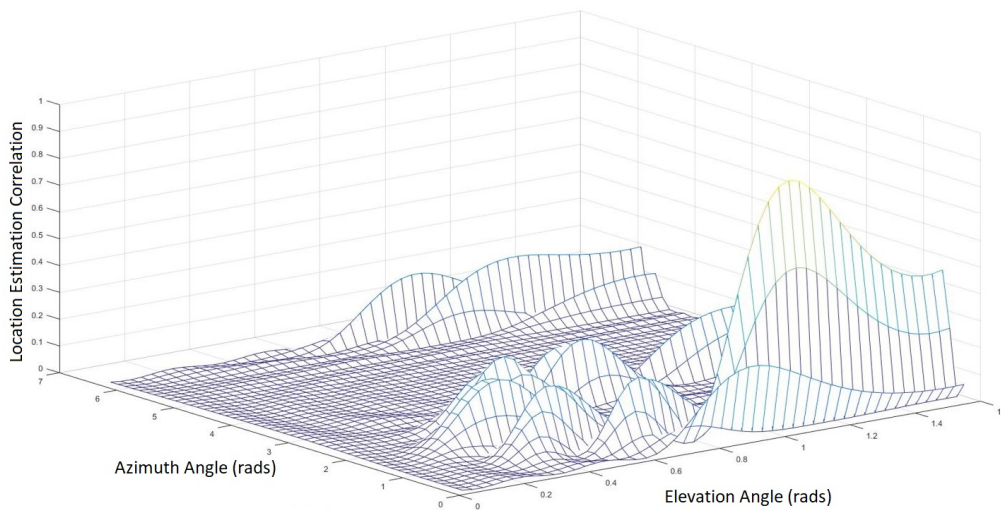


Figure 4.11: Correlation plot for coarse search.

Now, using the space selected from the coarse search, we run the direction finding algorithm again with a increased resolution of 200x200 points or more. The result obtained from this fine search will be more detailed and accurate than the ones obtained from past approaches. Figure 4.12 shows the correlation plot for fine search.

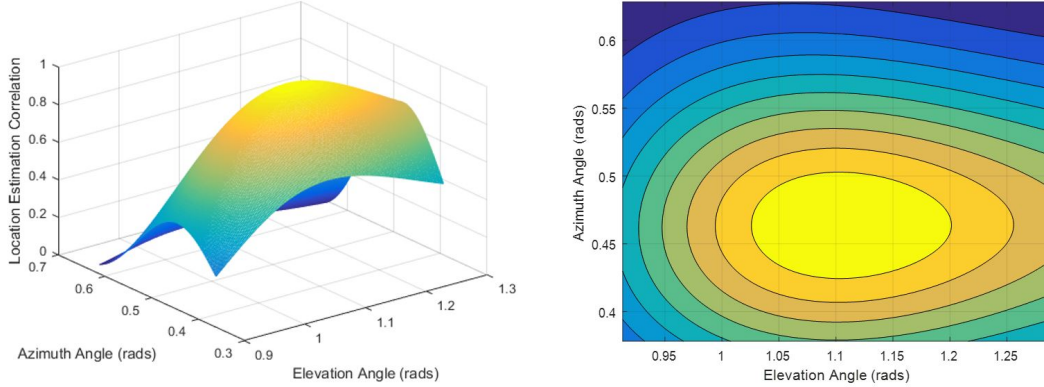


Figure 4.12: Correlation plot for fine search.

4.7.2 Interpolation approach

Even though the coarse search followed with a fine search improves the accuracy by a large margin, it is clearly visible that the computational time is increased when compared to the basic algorithm. In order for the algorithm to be used for practical purposes, both speed and accuracy matter. Hence, another approach to tackle this issue is using mathematical interpolation. This approach mainly relies on the fact that the antenna pattern for an antenna array is in the form of a parabola on a two-dimensional plot. In this interpolation model, first the coarse search is carried out with a maximum of 50×50 points. The point with maximum azimuth and elevation value is found from the coarse search. After that, four subsequent points, two on each azimuth plane and elevation plane are picked. Each of the two points in each plane are selected such that each point lies on either side of the point with maximum azimuth and elevation value. The selection is made so that the points have their correlation value in the range of -0.2 to $\text{max value} - 0.05$.

Now, as can be seen from the Figure 4.13, the general equation of the parabola can be given as $y = -(ax^2 + bx + c)$.

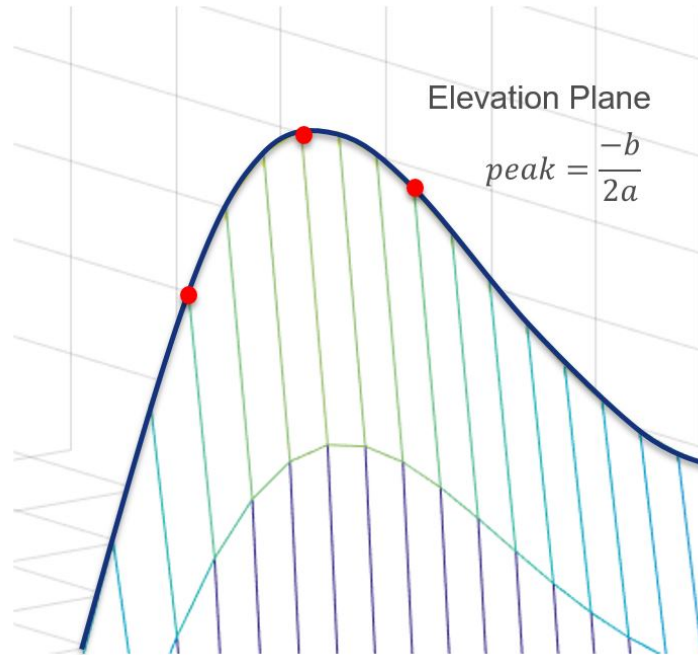


Figure 4.13: Inverted parabola.

Using the max value point, and the two points obtained on its both sides, equations of the two parabolas can be obtained for each azimuth and elevation plane. The peaks of these two intersecting parabolas give us the desired max azimuth and max elevation values. As it can be seen, this approach works on a very small resolution space, and uses the intersecting parabolas to find the maximum azimuth and elevation values, thus reducing the overall computational run time of the algorithm and improving accuracy.

Chapter 5

Evaluation

The first part of this chapter discusses the different Antenna Arrays used for this project, with varying geometrical arrangements and number of antennas. It is followed by a performance analysis of the proposed direction finding algorithm on multiple randomly generated test points. This also includes running the algorithm on the different antenna arrays. Results are compared to the ground truth value of the test points and also to the results obtained from the standard direction finding algorithm using planar sweep. Afterwards, the runtime of the algorithms on different processor cores is listed and discussed.

5.1 Antenna Array Geometry

On an antenna array, different antenna elements hear the signal a little earlier or later than others, measured by the phase of the signal. So, it is important to keep the time of arrival small in order to avoid large variations in the phase. Additionally, antenna geometry should be such that it favors line-of-sight (straight line from centre of antenna array to the target) with stellar accuracy in the cone under the antenna array. These conditions can easily be attained by using closed-loop antenna arrays where the antenna element separation is small, and phase difference can easily be accounted by utilizing the antenna geometries. Also, using closed-loop antenna arrays provides a cleaner antenna pattern with a larger main lobe and small side lobes.

Since this thesis is primarily aimed at antenna used in wireless Access Points, 5 different types of closed-loop antenna arrays with simple geometries were picked which are fairly common in the wireless industry and can be found in most commercially available

wireless Access Points. Their parameters were adjusted to simulate the real-world antenna geometries, having identical antenna separations (in feet) and mount height.

The antenna array geometries used are explained in section [5.1.1](#), [5.1.2](#), [5.1.3](#), [5.1.4](#), and [5.1.5](#).

5.1.1 Circular Array - 8 Elements

This is a circular antenna array with 8 antenna elements arranged uniformly around a circle of fixed radius as shown in Figure 5.1. For the sake of avoiding confusion with other circular arrays we will call this antenna array Circular8.

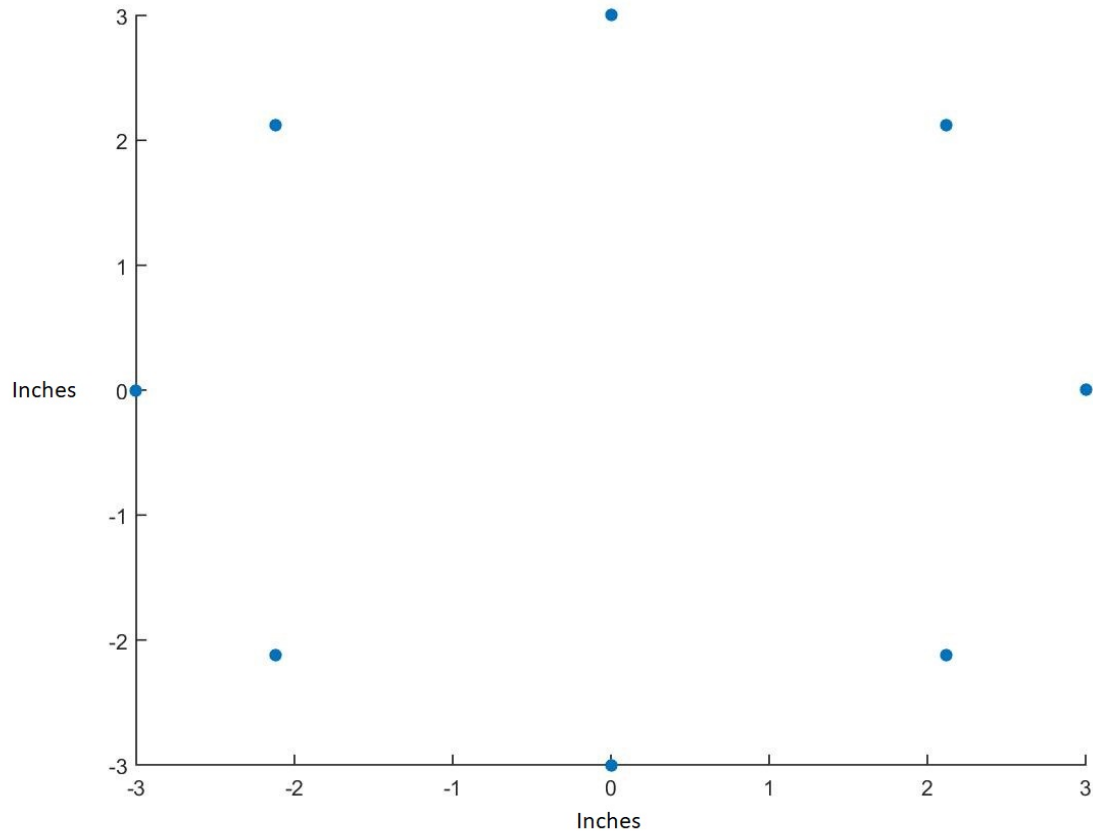


Figure 5.1: Circular Antenna Array - Circular8

5.1.2 Circular Ring Antenna Array - 16 Elements

A Circular Ring Antenna Array consists of two circular antenna arrays containing 8 antenna elements each. Both the arrays are offset by 90 degrees to each other as shown in Figure 5.2.

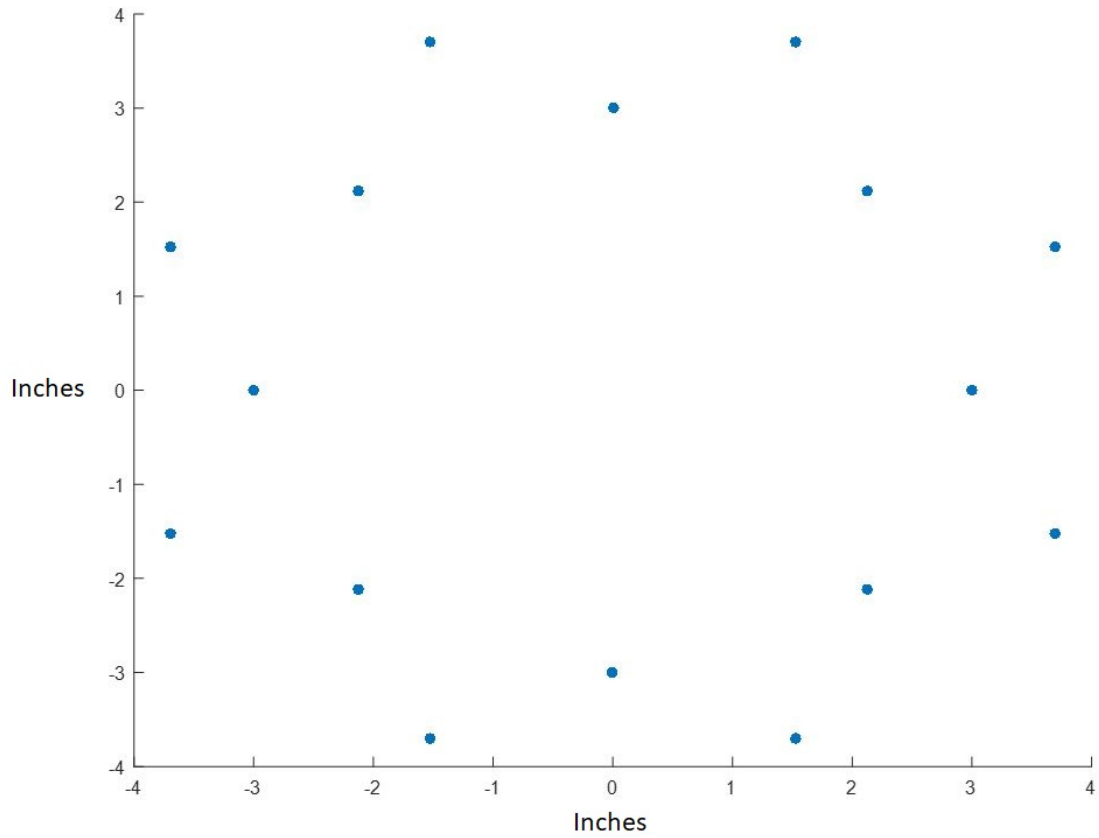


Figure 5.2: Circular Ring

5.1.3 Circular Antenna Array - 32 Elements

This is a circular antenna array with 32 antenna elements arranged uniformly around a circle of fixed radius as shown in Figure 5.3. For the sake of avoiding confusion with other circular arrays we will call this antenna array Circular32.

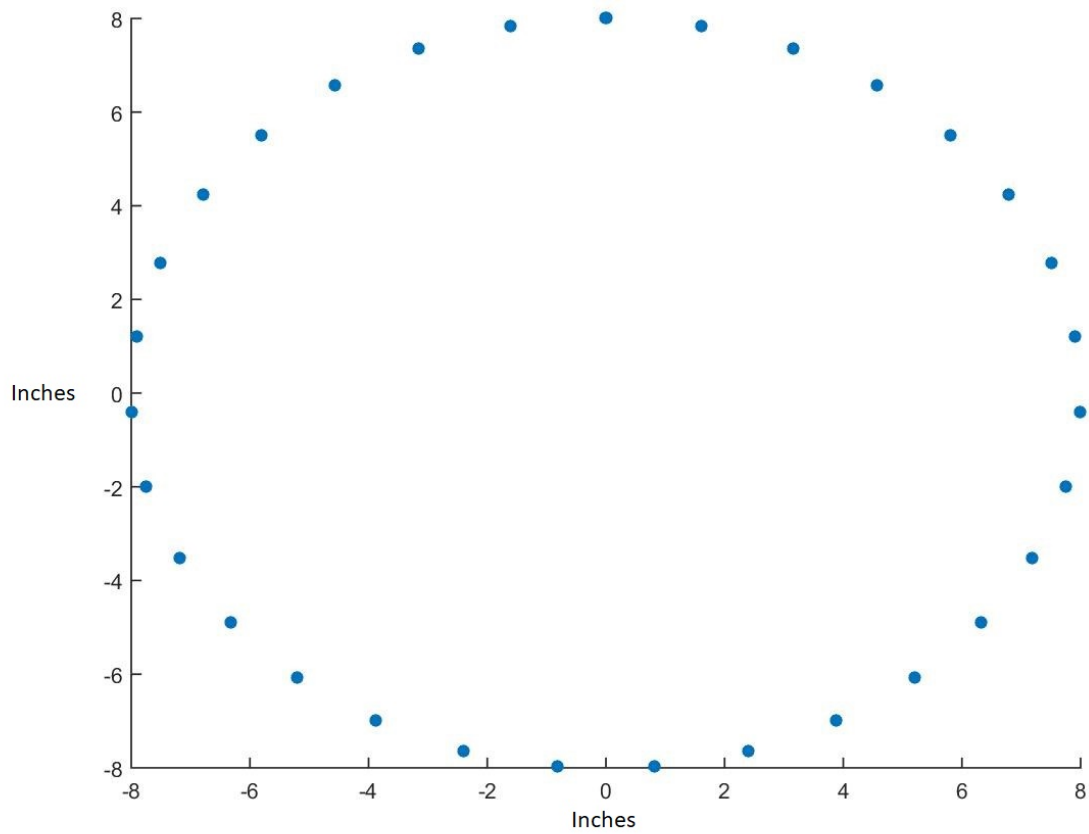


Figure 5.3: Circular antenna Array (Circular32)

5.1.4 Square Antenna Array - 16 Elements

The square antenna array has 16 antenna elements uniformly arranged on the sides of a square, with 4 antenna elements on each side. It is depicted as follows in Figure 5.4.

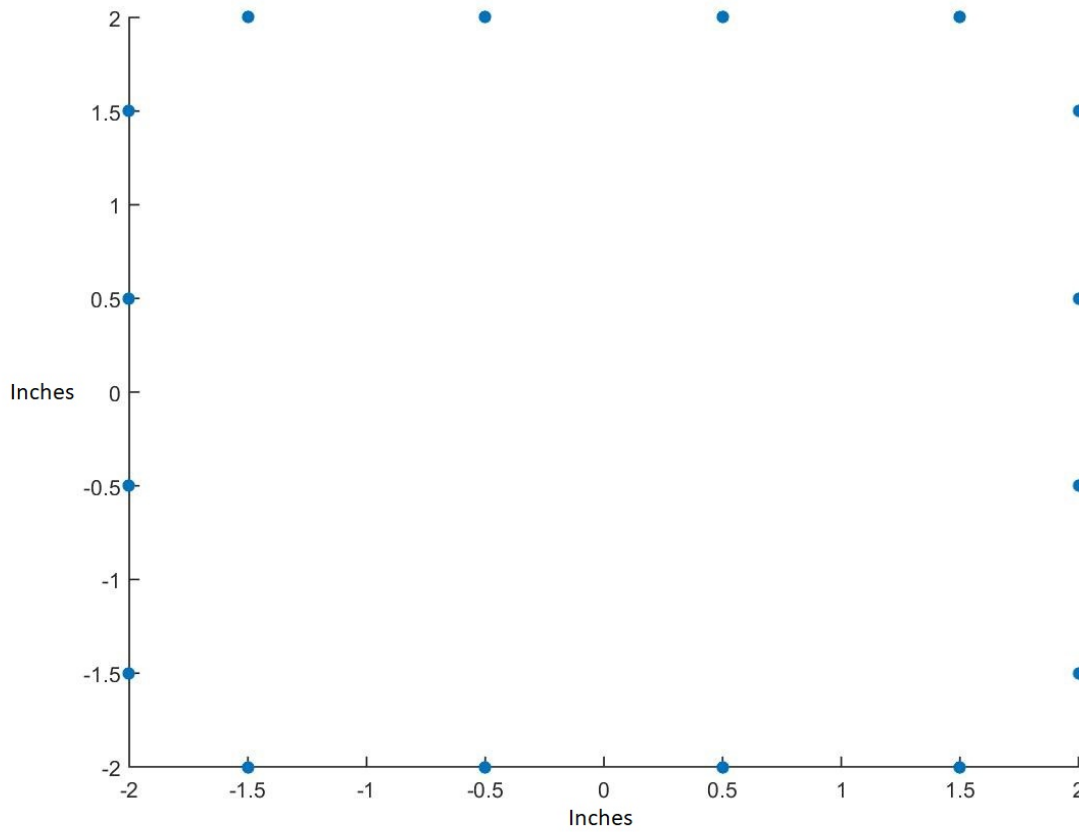


Figure 5.4: Square Antenna Array

5.1.5 Halo Antenna Array 32 Elements

The halo antenna is a square antenna array consisting of 32 different antennas, with 8 uniformly separated antennas on each edge of the square as shown in Figure 5.5.

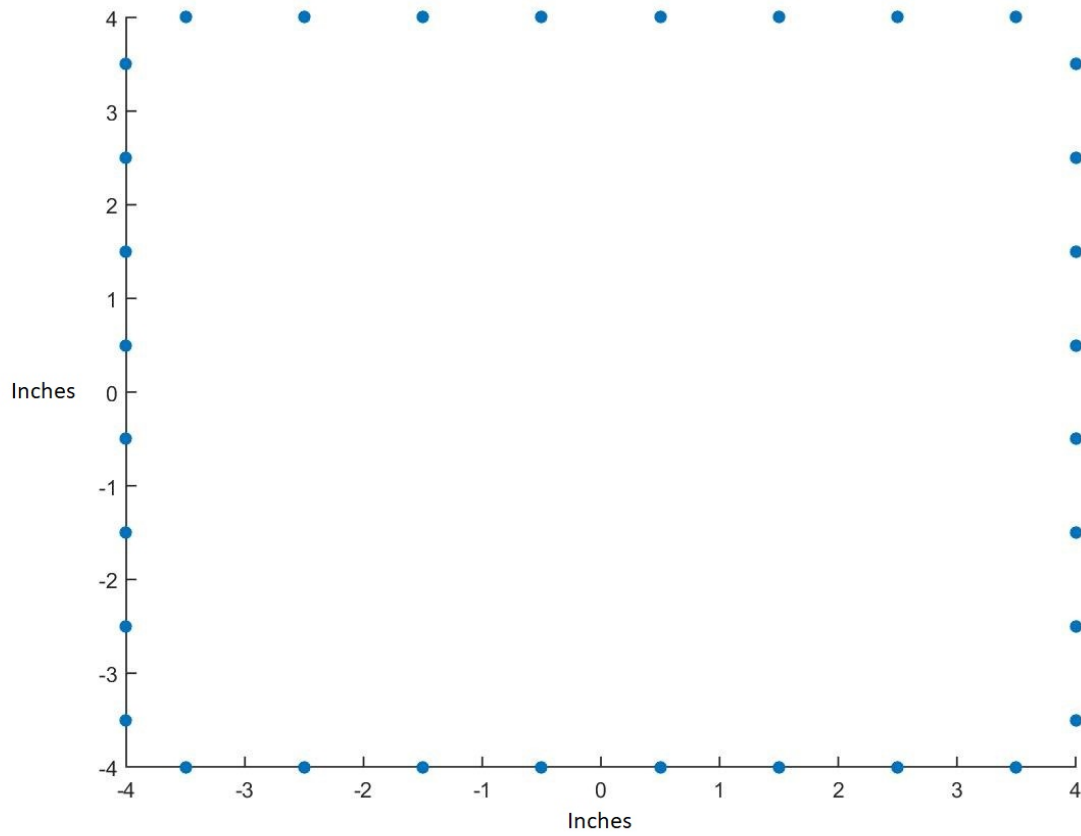


Figure 5.5: Halo Antenna Array

5.2 Performance Analysis

This section discusses the resultant azimuth angle and elevation angle, computed by the proposed direction finding algorithm using the interpolation method, for the randomly generated test points by using MATLAB random number generator. Being the conclusive solution for angle of arrival estimation suggested in this thesis, the interpolation method uses spherical sweep combined with coarse search, followed by curve fitting, to compute the angle of arrival. The resultant azimuth angle and elevation angles are then compared with the ground truth values of the test points in order to provide a measure for the algorithm's accuracy. Subsequently, the accuracy results are further compared with the results from the standard direction finding algorithm using planar sweep.

The algorithm is initially implemented in MATLAB. MATLAB uses a high-performance coding language, providing a mathematical computing environment. In this project, MATLAB was specifically used as it provides a simpler and cleaner way of visualising the location estimation correlation plots and the corresponding heatmaps produced by the direction finding algorithms, as opposed to other integrated development environments like Eclipse, Visual-Studio, Xcode, etc.

Since the conclusive role of the algorithm is to run on Wi-Fi routers or wireless Access Points, the parameters of the antenna arrays were set to match the parameters used in current modern Wi-Fi routers. Present routers are configured at a frequency of 5.18 GHz for the radio waves. Thus, the frequency parameter of the transmitted radio waves in the experiment set to 5.18 GHz. Radio waves are electromagnetic radiations and travel very quickly through space, moving slightly less than the speed of light. For this reason, the speed parameter of the waves was set at an approximate value of 300,000 km per second. The antenna array mount height was kept at 10 feet to simulate a Wi-Fi router mounted on the roof of an average household room. With the router being mounted on the center roof, the tests were carried out on a number of random test points, located on the floor of the room. Randomization of the test points was done to account for the degree of random variation in the input to the algorithm. The test points were generated using a random number generator with an upper threshold of 100 feet and lower threshold of -100 feet. Multiple instances of the test were carried out, using the same test point values, on different antenna array geometries.

Due to the interpolation algorithm performing a coarse search, it was run with a sweep resolution of 50x50 points, or a total of 2,500 points. To achieve an accuracy of less than 1 meter, the percentage error between the resultant values from the algorithm and the ground truth values should be less than 25%. Having more than a variation of 25% from

the ground truth, in both the azimuth and elevation angles, causes the resultant location of the test point to be off by nearly 3.2 feet or 1 meter, thereby, making the algorithm undesirable towards a hyperlocation solution. The antenna geometries used are all closed-loops antenna arrays with similar geometries. Thus, they should generate similar results for a given test point value.

Table 5.1 presents a comparison of the resultant azimuth angle from the interpolation algorithm to the ground truth values for different test points, on different antenna array geometries. At the bottom of the table, average percentage error in the computed azimuth value to the ground truth value is listed.

Test Point	Mount Height	Azimuth Angle (in radians)					
		Ground Truth	Halo	Square	Circular32	Circular Ring	Circular8
20, 10	10	0.46364	0.50470	0.47423	0.54308	0.47735	0.47023
-35, 69	10	2.04022	2.06511	2.04386	2.06290	2.04781	2.04534
78, 15	10	0.18998	0.19939	0.19039	0.21879	0.19290	0.19112
21, 44	10	1.12549	1.17838	1.13061	1.19035	1.13927	1.13456
31, -30	10	5.51420	5.56188	5.52029	5.59073	5.53099	5.52348
-26, -57	10	4.28440	4.32692	4.28860	4.32572	4.29570	4.29199
38, 17	10	0.42066	0.43215	0.42286	0.43808	0.42477	0.42344
02, -09	10	4.93110	4.93711	4.93259	4.97953	4.93457	4.93343
51, -23	10	5.85950	5.91425	5.86270	5.95312	5.87796	5.86579
-90, -88	10	3.91020	3.94443	3.91517	3.94943	3.92113	3.91757
Average % Error			2.62532	0.40857	4.92542	0.83070	0.44330

Table 5.1: Comparison between azimuth angle values computed using interpolation method for different antenna arrays.

Similarly to Table 5.1, Table 5.2 presents a comparison of the resultant elevation angle from the interpolation algorithm to the ground truth values for different test points, on different antenna array geometries. At the bottom of the table, average percentage error in the computed elevation value to the ground truth value is listed.

Test Point	Mount Height	Elevation Angle (in radians)					
		Ground Truth	Halo	Square	Circular32	Circular Ring	Circular8
20, 10	10	1.15026	1.12081	1.17315	1.12135	1.13475	1.16140
-35, 69	10	1.44225	1.48562	1.48571	1.47765	1.48563	1.48567
78, 15	10	1.44555	1.46952	1.48378	1.47435	1.48390	1.48394
21, 44	10	1.36849	1.43109	1.44067	1.34355	1.44043	1.44057
31, -30	10	1.34301	1.38460	1.40255	1.32186	1.40220	1.40242
-26, -57	10	1.41251	1.46458	1.46669	1.43973	1.46656	1.46663
38, 17	10	1.33504	1.35657	1.37422	1.32982	1.37376	1.37403
02, -09	10	0.74481	0.72203	0.72222	0.72184	0.72213	0.72218
51, -23	10	1.39392	1.44358	1.44839	1.39553	1.44813	1.44824
-90, -88	10	1.49196	1.50708	1.50710	1.50407	1.50709	1.50709
Average % Error			2.78311	3.20843	1.66853	3.13502	3.10295

Table 5.2: Comparison between elevation angle values computed using interpolation method for different antenna arrays.

From both Table 5.1 and 5.2, it can be seen that the azimuth angle and elevation angle values obtained from the proposed algorithm using interpolation method are very close to the ground truth values for respective test points. Even with varying antenna array geometries, the results stay consistent. The average percentage error for the azimuth angle is in the range of 0.4% to 4.9%, and for the elevation angle is in the range of 1.6% to 3.2%. Both the deviations in the percentage errors are quite small and less than the 25% threshold. Thus, the accuracy of the location calculated by the interpolation method lies within the 1-meter range of the original test point, making it a suitable candidate for hyperlocation.

Also, it can be observed that, for a particular type of antenna array geometry, the percentage error in azimuth angle tends to decrease with the decreasing number of antennas, while the percentage error in elevation angle tends to increase with the decreasing number of antennas. From the array factor of a circular array, as described in section 4.2.4, it can be seen that by using a spherical sweep for a test point located parallel to the plane of the antenna geometry, that is, the azimuth plane, the antenna radiation pattern tends to be more directional towards the azimuth side with fewer elements in the antenna array. On increasing the number of elements in the antenna array, the directionality of the antenna starts moving to the elevation side.

Now, in order to show that the proposed algorithm is less computationally expensive than the standard direction finding algorithm using planar sweep, the latter algorithm was run on the same test points with two different sweep resolutions. The first resolution used was 200x200 points for sweep on each plane, thus, making the total sweep resolution (for

two sweeps) to be 80,000 points. The second resolution used was kept to match that of the interpolation method, that is, 50x50 points for sweep on each plane, thus, making the total sweep resolution (for two sweeps) to be 5,000 points.

Table 5.3 shows the resultant azimuth angle and elevation angles from the standard direction finding algorithm using planar search with a resolution of 200x200 points, 50x50 points.

Results using Planar sweep method on Halo (in Radians)							
Test Point	Mount Height	Ground Truth		200x200		50x50	
		Azimuth	Elevation	Azimuth	Elevation	Azimuth	Elevation
20, 10	10	0.46364	1.15026	0.46364	1.15026	5.0302	1.26805
-35, 69	10	2.04022	1.44225	2.19265	1.40170	4.8280	1.39235
78, 15	10	0.18998	1.44555	0.19000	1.44560	4.9805	1.45380
21, 44	10	1.12549	1.36849	1.12540	1.36849	5.3646	1.28945
31, -30	10	5.5142	1.34301	5.51420	1.34301	5.2719	1.40122
-26, -57	10	4.2844	1.41251	4.12440	1.36060	4.1062	1.35506
38, 17	10	0.42066	1.33504	0.43190	1.35439	5.7013	1.35439
02, -09	10	4.9311	0.74481	4.93110	0.74481	4.7779	1.25460
51, -23	10	5.8595	1.39392	5.85950	1.39392	5.6817	1.41051
-90, -88	10	3.9102	1.49196	3.63980	1.47450	3.6140	1.47325
Average % Error				2.08114	0.91097	529.74	10.0787

Table 5.3: Comparison of both azimuth and elevation angle generated by planar sweep using resolution 200x200 and 50x50.

On looking at the values from Table 5.3, it can be seen that the standard direction finding algorithm using planar sweep gives percentage error for both azimuth angle and elevation angle within the 25% accuracy range when used with a resolution of 200x200 points. However, on decreasing the number of points to 50x50, the percentage error is computed to be an incredibly large value of 530% for the azimuth angle. This is due to the fact that on decreasing the resolution for planar sweep, the region containing the main lobe of the antenna radiation pattern gets omitted, and the algorithm returns azimuth and elevation values based on the side lobes, which are contained in the search resolution. Hence, it can be concluded that the standard direction finding algorithm using planar sweep needs to use a larger resolution in order to be effective, making the interpolation algorithm, which uses a considerably smaller resolution, relatively less computationally intensive.

5.3 Runtime Comparison

Runtime, also known as execution time, refers to the duration which the processor takes in order to execute a program or the time during which a program is said to be running. Every software establishment aims at achieving shorter runtime for their code for speedy program executions, better memory management, and faster freeing of hardware resources. Shorter runtime is generally associated with things like faster CPUs, multi-threading, etc.

The main objective of the proposed interpolation algorithm is to allow running of complex direction finding algorithms on weaker processor cores, specifically in the Wi-Fi routers, without sacrificing speed and efficiency. Generally, CPU cores in small devices like routers, access-points, etc. are single core processors with processing speed ranging from 500 MHz to 1.5 GHz. Having only single cores, it is not possible to spread the processing task among different processors to make the execution of the program faster. Thus, in this scenario, clock speed matters more than parallelism. However, some of the CPU units are equipped with a DSP core. A DSP core is a specialized microprocessor, designed specifically for Digital Signal Processing. This DSP core can be utilized for handling the computations without involving the use of the main processing unit thus reducing the overall runtime.

From the previous discussion, it can be seen that the interpolation approach is quite accurate with small error margins, even with varying antenna array geometries. Now, to measure the runtime comparisons, the algorithm was run on three different CPU units: 14 nm “Broadwell” 2.5 GHz Intel “Core i5” processor (5257U), 1.2 Ghz Cortex-A53 ARMv8 CPU, 1.2 Ghz Cortex-A53 ARMv8 with NEON DSP. For having a consistent measure of comparison between all the CPUs, the code was re-written in C language using basic C libraries present in the GNU Compiler Collection (GCC). The operating system used is Raspbian GNU/Linux version 8.0, April 2016 build. For consistency, the Halo antenna array was used. For all the CPUs, the algorithm was run using single core.

To utilise the DSP unit, an external library had to be deployed. It is called the NE10 library and is a part of an open source optimized software library project for the ARM architecture. Ne10 is a library of common, useful functions that have been heavily optimised for ARM-based CPUs equipped with NEON SIMD capabilities. It is a translation of Assembly code to C functions. The library provides some of the fastest open source implementations of key operations available for the ARM v7-A and v8-A architectures, particularly focusing on math, signal processing, image processing, and physics functions [1].

Table 5.4 shows the performance matrix for runtimes on different CPUs for 1000 cycles of the direction finding algorithms with planar sweep and interpolation. Cycles refer to

the number of times the algorithm was run in a given time period. Similar results with variations less than 10 ms were obtained upon multiple iterations of the experiment.

PLATFORM	PLANAR SWEEP - Runtime (1000 cycles)	INTERPOLATION - Runtime (1000 cycles)
INTEL CPU (2.5 GHz)	90 ms	30 ms
ARM CPU (1.2 GHz)	720 ms	140 ms
ARM + NEON DSP (1.2 GHz)	450 ms	55 ms

Table 5.4: Runtime comparison between planar sweep and interpolation algorithm on different processing units.

From the Table 5.4, it can be seen that the interpolation algorithm is significantly faster than the planar sweep algorithm. This is mainly due to the fact that the sweep area for one cycle of planar sweep is over 80,000 points in space and is only 2,500 points for interpolation method. So, the amount of calculations performed decreases substantially. Also, the impact of utilising DSP cores in the ARM CPU can be clearly seen, with the runtime increasing to almost double the value without the DSP unit.

Chapter 6

Conclusion

This thesis presented an overview of the most commonly used and upcoming direction finding methodologies in the industry. Methods for finding the angle of arrival that were discussed aimed at determining the angle of arrival by making an estimation of the azimuth and elevation angles for an incident signal at the antenna arrays. However, most of the methods were not able to associate the two angle parameters together and in addition some of them needed a known signal transmit sequence to perform the correlation function for computing the angle of arrival. Algorithms like Capon, MUSIC or even CALS encounter drawbacks like the load of mathematical calculations, the imprecision of the results, or the need for some information about the transmitted signal or other characteristics of the transmission channel. Thus, the thesis laid focus on the angle of arrival algorithm using correlative interferometry, which posed the least restrictions in the context of providing a hyperlocation solution.

The main objective of this thesis was to improve upon the existing angle of arrival estimation algorithm using correlative interferometry principle in a way to reduce the overall computation load, and thereby, making the algorithm to be able to run on weaker processing units with a respectable runtime.

In this thesis, the method of estimating angle of arrival using correlative interferometry was studied in detail and areas were focused where the improvements could be suggested. It was observed that the heavy search resolution for finding vector correlations could be reduced by a considerable amount by making use of a spherical coordinate system instead of cartesian coordinate system. Also, the lookup time for finding the maximum correlation angle could be further reduced by using mathematical interpolation or curve fitting by using the parabolic nature of the antenna array radiation pattern. Consequently, the

computational complexity of the proposed algorithm was much smaller than the original algorithm to estimate the angle of arrival.

Based on the comparison results between the original algorithm using correlative interferometry and the proposed solution, the precision of the two algorithm was found to be nearly identical, with less than 5% error. Additionally, the proposed solution gave substantially faster runtimes on weaker processing units when compared to the original solution.

Hence, in conclusion, the proposed solution looks very promising as an alternative to the original algorithm using correlative interferometry for obtaining better runtimes on weaker processing units of wireless access points and coupled with some efficient bearing-only location algorithm can generate superior results to any existing direction finding method; thus, providing an effective hyperlocation solution.

6.1 Future Work

The current thesis aimed to improve the runtime for angle of arrival estimations on weaker processing units containing single core processors. The algorithm could be further advanced by distributing the workload of computing the vector correlations on multiple processors. This will allow for an increase in the resolution space while maintaining the runtime.

Furthermore, the algorithm could be paired with bearing-only location algorithms to form core hyperlocation unit. The angle of arrival can be computed by multiple processors for a given client device and the data can be collected by a central unit or cloud and can be worked on further using a bearing-only algorithm thus forming a core hyperlocation unit. For instance, the angle of arrival can be computed by multiple access points for a given client device and the data can be collected and transmitted to a master access point to provide even more fine-grained location results. Also, the algorithm can be modified to work using the Bluetooth Low Energy (BLE) technology to provide location estimates. Since BLE units have weaker processing power, the proposed algorithm would be able to fare better than most of the direction finding algorithms.

References

- [1] Project Ne10: An open optimized software library project for the ARM architecture. <https://projectne10.github.io/Ne10/>. Accessed: 2016-08-28.
- [2] M. T. Brenneman and Y. T. Morton. A novel maximum likelihood estimator for gps signal angle of arrival. In *proceedings of the 43rd Asilomar Conference on Signals, Systems and Computers*, pages 1154–1158, Pacific Grove, CA, USA, 2009.
- [3] B. F. Burke and F. Graham-Smith. *Introduction to Radio Astronomy: 2nd edition*. Cambridge University Press, Cambridge, UK, 2002.
- [4] T. Chai and R. R. Draxler. Root mean square error (RMSE) or mean absolute error (MAE)? Arguments against avoiding RMSE in the literature. *Geoscientific Model Development (GMD)*, 7(3):1247–1250, 2014.
- [5] K. R. Dandekar, H. Ling, and G. Xu. Effect of mutual coupling on direction finding in smart antenna applications. *Electronics Letters*, 36(22):1889–1891, 2000.
- [6] B. T. Fang. Simple solutions for hyperbolic and related position fixes. *IEEE Transactions on Aerospace and Electronic Systems*, 26(5):748–753, 1990.
- [7] Xiaoming Gou, Y. Xu, Z. Liu, and X. Gong. Capon beamformer for acoustic vector sensor arrays using biquaternions. In *proceedings of the 3rd International Conference on Awareness Science and Technology (iCAST)*, pages 28–31, Dalian, China, 2011.
- [8] G. Hislop, N. Sakar, and C. Craeye. Direction finding with MUSIC and CLEAN. *IEEE Transactions on Antennas and Propagation*, 61(7):3839–3849, 2013.
- [9] S. Imai, K. Taguchi, and T. Kashiwa. Direction of arrival estimation in FDTD analysis of radio propagation using MUSIC method. In *proceedings of the 12th International Symposium on Antennas and Propagation (ISAP)*, pages 1–2, Hobart, TAS, Australia, 2015.

- [10] A. Khallaayoun, R. J. Weber, and Y. Huang. A blind iterative calibration method for high resolution DOA estimation. In *proceedings of the 19th Military Communications Conference (MILCOM)*, pages 199–204, Baltimore, MD, USA, 2011.
- [11] J. Litva and T. Kwok-Yeung Lo. *Digital beamforming in wireless communications*. Artech House Boston, MA, USA, 1996.
- [12] X. Long, S. M. A. Salehin, and T. D. Abhayapala. Robust Capon beamformer with frequency smoothing applied to medical ultrasound imaging. In *proceedings of the 16th IEEE Workshop on Statistical Signal Processing (SSP)*, pages 173–176, Gold Coast, VIC, Australia, 2014.
- [13] Z. X. Lu, M. G. Gao, and Y. J. Li. Robust Capon beamformer based on direction search. *Electronics Letters*, 48(23):1472–1473, 2012.
- [14] M. Malajner, P. Planinsic, and D. Gleich. Angle of arrival estimation using RSSI and omnidirectional rotatable antennas. *IEEE Sensors Journal*, 12(6):1950–1957, 2012.
- [15] S. Mirchandani, C. Rawat, A. Krishnan, A. Agarwal, G. Isola, and V. Sivaprasad. Maximum likelihood angle of arrival estimation using least mean squares technique. In *proceedings of the 9th International Conference on Emerging Trends in Robotics and Communication Technologies (INTERACT)*, pages 129–132, Chennai, India, 2010.
- [16] Cisco White Paper. Antenna patterns and their meaning. http://www.cisco.com/c/en/us/products/collateral/wireless/aironet-antennas-accessories/prod_white_paper0900aecd806a1a3e.html. Accessed: 2016-10-21.
- [17] Cisco White Paper. Cisco visual networking index: Forecast and methodology. <http://www.cisco.com/c/en/us/solutions/collateral/service-provider/visual-networking-index-vni/complete-white-paper-c11-481360.html>. Accessed: 2017-02-15.
- [18] S. Pillai and F. Haber. Statistical analysis of a high resolution spatial spectrum estimator utilizing an augmented covariance matrix. *IEEE Transactions on Acoustics, Speech, and Signal Processing*, 35(11):1517–1523, 1987.
- [19] K. Rao, A. Singh, and S. Singh. Novel design and implementation of base line interferometry direction finding BLI DF algorithm. *International Journal of Electronics and Communication Engineering (SSRG - IJECE)*, 1(8):29–35, 2014.

- [20] A. D. Redondo, T. Sanchez, C. Gomez, L. Betancur, and R. C. Hincapie. MIMO SDR-based implementation of AOA algorithms for radio direction finding in spectrum sensing activities. In *proceedings of the 8th IEEE Colombian Conference on Communication and Computing (COLCOM)*, pages 1–4, Popayan, Colombia, 2015.
- [21] E. Silva, S. O’Connor, and C. Massa. The beacon locator project: A passive direction finding system for locating pulsed emitter signals. https://web.wpi.edu/Pubs/E-project/Available/E-project-101711-123941/unrestricted/Beacon_Locator_Report.pdf. Accessed: 2016-11-09.
- [22] Cisco Systems. Cisco hyperlocation module with advanced security data sheet. http://www.rohde-schwarz-ad.com/docs/ewtest/intro_theory_of_direction_finding.pdf. Accessed: 2017-05-02.
- [23] Cisco Systems. Wi-fi location-based services 4.1 design guide. <http://www.cisco.com/c/en/us/td/docs/solutions/Enterprise/Mobility/WiFiLBS-DG/wifich2.html>. Accessed: 2017-02-11.
- [24] C. C. Teague. Root-MUSIC direction finding applied to multifrequency coastal radar. In *proceedings of the 22nd IEEE International Geoscience and Remote Sensing Symposium*, volume 3, pages 1896–1898 vol.3, Toronto, ON, Canada, 2002.
- [25] H. Tian, S. Wang, and H. Xie. Localization using cooperative AOA approach. In *proceedings of the 3rd International Conference on Wireless Communications, Networking and Mobile Computing*, pages 2416–2419, Shanghai, China, 2007.
- [26] A. V. Tondwalkar and P. Vinayakray-Jani. Terrestrial localization by using angle of arrival measurements in wireless sensor network. In *proceedings of the 9th International Conference on Computational Intelligence and Communication Networks (CICN)*, pages 188–191, Jabalpur, India, 2015.
- [27] V. I. Vasylyshyn. Direction finding using bank of modified weighted unitary root - MUSIC estimators. In *proceedings of the 2nd IEEE Microwaves, Radar and Remote Sensing Symposium (MRRS)*, pages 18–21, Kiev, Ukraine, 2014.
- [28] G. Xu and T. Kailath. Direction-of-arrival estimation via exploitation of cyclostationary - a combination of temporal and spatial processing. *IEEE Transactions on Signal Processing*, 40(7):1775–1786, 1992.
- [29] Lianqing Yu, Ning Wang, Huan Zhu, Yi Chen, and Tao Jiang. Simulation research to finding direction precision based on music algorithm in non-uniform circular array. In

proceedings of the 16th IEEE International Conference on Communication Technology (ICCT), pages 142–146, Hangzhou, China, 2015.

- [30] D. Zachariah, M. Jansson, and S. Chatterjee. Enhanced Capon beamformer using regularized covariance matching. In *proceedings of the 5th IEEE International Workshop on Computational Advances in Multi-Sensor Adaptive Processing (CAMSAP)*, pages 97–100, St. Martin, France, 2013.